Spring 6-10-2023

Spatiotemporal dynamics of ticks and tick-borne disease at NEON sites across a sub-continental scale

Ana Sofia Rivera
DePaul University, ARIVER79@depaul.edu

Spatiotemporal dynamics of ticks and tick-borne disease at NEON sites across a sub-continental scale

A Thesis

Presented in partial fulfillment of the requirements.

For the Degree of Master of Science

June 2023

BY

A. Sofia Rivera

Department of Biological Sciences

College of Science and Health

DePaul University

Chicago, IL

Acknowledgements

I am grateful for all the people that made this possible and gave me the support throughout this journey with words of encouragement. I would like to give special thanks to my family who helped me push through rough moments. My parents who gave me the access for a higher education and gave me the support emotionally and financially; to Sonia, who played the role as a mom giving me advice and helping me become a better person and a better scientist; to Manuel, my oldest brother, who I look up to due to his professional and personal success; to Andrea, who always supported me in every decision without hesitation; to Eddy and Daniel, who them being scientist always offered help and gave me a better perspective of life; to Mac, my cat, who helped me manage my time and take breaks. I give a great thanks to DePaul University, where I learned from great researchers and faculty. It was a pleasure to be part of a great community for so many years. I owe a great thank you to my advisor, Dr. LaMontagne, who helped me achieve my goals and supported me since undergraduate. Finally, I would like to acknowledge the National Ecological Observatory Network who provided me with the data and instructed me during the analysis. I hope the significance of my research will be of value for future research addressing questions related to tick outbreaks and tick-borne diseases.

Table of Contents

Abstract
Tick-borne diseases in humans such as Lyme disease cases in the United States have doubled between 2004 and 2016. Understanding the dynamics of infectious diseases has long been of interest for ecologists. Tick and tick-borne diseases are influenced by temperature and precipitation at local scales, indirectly through mast seeding in forest trees which increases the abundance of tick hosts (e.g., small mammals). Most tick studies occur at local scales that comprise only a small part of their range. The aim of my thesis is to characterize spatiotemporal dynamics of ticks and tick-borne diseases in the eastern United States. I used datasets from National Ecological Observatory Network (NEON) from 2014 to 2021 to quantify the level of synchrony in tick dynamics in seven NEON Domains, representing different ecoregions, and spanning distances up to 2,000 km. I used multiple regression matrices (MRM) to examine patterns of synchrony across sites in regional to sub-continental patterns of host-seeking ticks, and climatic variation. I found that spatial synchrony in temporal patterns of nymph abundance for both *Amblyomma americanum* and *Ixodes scapularis* declined with increasing distance between NEON sites. Weather variables associated with the spatiotemporal dynamics and key predictors of ticks and tick-borne diseases vary between the two species. *A. americanum* nymoh abundance was driven by lags in July temperature differences, ΔT_3 (difference in mean July temperatures in year t-3 and t-4) and ΔT_4 (difference in mean July temperatures in year t-4 and t-5); and January conditions impacted tick survival for *I. scapularis*. The proportion of nymph-infected ticks was explained by environmental factors for *A. Americanum*, whereas it was not for *I. scapularis*. Nymph abundance and the tick-borne diseases could be understood by identifying environmental variables influencing tick spatiotemporal patterns.

List of Tables

List of Figures

List of Appendices

Chapter I – Introduction

Zoonotic diseases represent a threat to global health and their dynamics are driven by environmental factors (Jones et al., 2008). More than 60% of zoonotic diseases that affect humans are caused by pathogens shared with wild or domestic animals (Karesh et al., 2012; Ostfeld et al., 2018). The emergence of zoonotic diseases can be directly related to ecosystem disruption, such as land use, extraction of natural resources, animal production systems, modern transportation, antimicrobial drug use, and global trade (Karesh et al., 2012). Ecosystem disruption allows the growth of pathogens affecting the incidence of zoonotic diseases, increasing cross-species transmission, including tick-borne diseases.

There are two families of ticks that are capable of transmitting pathogens to humans, they are the Ixodidae, or hard ticks, and the Argasidae or soft ticks (Spach et al., 1993). The family Ixodidae is of significant medical and veterinary importance (de la Fuente et al., 2017). Ixodidae ticks undergo four life stages during their two-year lifespan: egg, larva, nymph, and adults, and the nymphal stage is when infection of the host occurs and is the stage most likely to infect humans (LoGiudice et al., 2003). The Ixodidae family includes the genera *Ixodes, Dermancentor,* and *Amblyomma*. These species are responsible for transmitting some of the most prevalent and widespread infections to humans such as Rocky Mountain spotted fever transmitted by *Dermancetor*; Lyme disease transmitted by the *I. scapularis*; and ehrlichiosis, transmitted by *A. americanum* and *I. scapularis* (Swei et al., 2020).

Ticks and tick-borne pathogens in the United States

Tick-borne diseases have been a great concern since the 19th century due to their fast-expanding rates over space and time (Eisen et al., 2017). Some diseases such as Lyme disease have been known for many years in their endemic areas, however their geographic range has expanded and occurring in new countries which has increased since the mid-1990s (Kugeler et

al, 2015; Eisen et al., 2017). Even though ticks present a great concern currently, tick and tick-borne diseases have been detected in human tissues from over 5,300 years ago (Dubrey et al., 2014).

Ticks can transmit a wide diversity of pathogens to their hosts, including protozoa, bacteria, and viruses. *Ixodes scapularis* is mostly recognized for transmitting *Borrelia burgdorferi*, a bacterium that is the cause of Lyme disease, named after the town of Lyme in Connecticut, USA, and was first detected in the 1980s (Burgdorgfer et.al, 1982). The spirochete named *B. burgdorferi* was named after Willy Burgdorfer who found the connection between *I. scapularis* and Lyme disease. Even though Lyme disease was described in understanding of the illness in 1975, it was not until 1982 that *B. burgdorferi,* and 2016, *B. mayonii*, as the etiological agents were described (Eisen et al., 2017). Cases of Lyme disease in the United States were first reported in Wisconsin and Southern Connecticut due to common symptoms, such as paralysis, fatigue, and the common skin rash called erythema migrans (Burgdorgfer et.al, 1982).

Amblyomma americanum was first described in 1754 in the United States; and in 1986 pathogens were documented. Cases have been mainly reported from southern states, as a common disease known as Ehrlichiosis transmitted by *Ehrlichia chaffeensis* and *Ehrlichia ewingii* (Mixson et al., 2006). This disease is known by prolonged febrile illness, exposing fever, chills, and headache often accompanied with nausea, myalgias, arthralgias, and malaise. Even though this disease is expanding, patients have presented prolonged illnesses due to lack of consideration in diagnosis (Roland et al., 1995). However, this pathogen has expanded northwards and is detected in regions in the northeastern United States (Mixson et al., 2006). Tick-borne diseases and their rapid expansion have become a great concern in public health.

Ticks and their hosts

Ticks detect their hosts by detecting breath and odors; they pick a place to wait for a host such as the tips of grasses, shrubs, leaf litter or twigs near the ground (CDC, 2020; Eisen et al., 2017). When the host brushes the spot, the tick climbs onto the host. For *I. scapularis*, white-footed mouse (*Preomyscus leucopus)* and the western tree squirrel (*Sciurus griseus*), are highly competent reservoir hosts for *B. burgdorferi* (Eisen et al., 2017). For *A. americanum*, its distribution has been related to increasing densities of its principal host, white-tailed deer and wild turkeys (*Meleagris gallopavo*). Although tick abundance for *I. scapularis* has been highly associated with white-tailed deer (*Odocoileus virginianus*), white-tailed deer is an incompetent reservoir for pathogens for *B. burgdorferi*. The white-tailed deer serves as a primary reproductive stage host serving as a blood meal source for gravid female ticks (Rand et al., 2003). However, for some pathogens (e.g., *Erlichiosis* spp.) transmitted by *A. americanum*, white tailed deer are considered the main reservoir host (Paddock & Yabsley, 2007). Due to species interactions, research focusing on the reduction of ticks as a disease vector has included hunting of deer to reduce tick numbers; however, this measure is not effective for a reduction of tick abundance and tick pathogens (Granter et al., 2014; Paddock & Yabsley, 2007). Factors influencing tick abundance is the availability of host, and in turn host availability is connected to food resources, such as tree seed abundance (e.g., acorns) (Janzen, 1971; Ostfeld et al., 2001; Elkinton et al., 2004; Granter et al., 2014; Ostfeld et al., 2018). Oaks, and many other tree species have a characteristic synchronous pattern of reproduction that is highly variable over time, known as mast seeding (Silvertown 1980). The enormous production of seed during a mast event is an excellent food resource for many species of seed-eating small mammals (Granter et al., 2014; Ostfeld et al., 2001). Mast seeding is a resource pulse, a rare event with short duration

and high magnitude. Mast seeding drives the dynamics of plant and animal population (Yang et al. 2008) and influences population growth for seed predators that feed directly on the seed crop such as seed-eating small mammals (Kelly et al., 2008), therefore influencing the spatiotemporal distribution of ticks, who feed mainly from hosts such as the white-footed mouse, the eastern chipmunk, the western tree squirrel, and deer. Mast-seeding dynamics, small mammal abundance, tick abundance, and tick-borne diseases have all been linked with climate variables. Since ticks spend 95% of their life off host and on the forest floor, they are exposed to environmental conditions, particularly temperature and precipitation (Ostfeld et al., 2006, 2018, 2001; Kelly, 2008). By understanding environmental variables influencing tick spatiotemporal patterns and the emergence of tick-borne diseases, ecologists and epidemiologists have the possibility to predict the emergence and spread of ticks and tick-borne diseases by understanding their dynamics of transmission and abundance.

Risk of infection with a tick-borne pathogen and exposure to ticks varies on local and regional scale, since they attach to hosts and move larger distances with respect to the movement distances of ticks, typically <1 m (Ostfeld et al., 1995). Present literature on ticks and tick-borne pathogen dynamics tends to be limited in geographic area, the focus being the northeastern United States (Ostfeld et al., 2001, 1995; Hayes et al., 2015; Horobik et al., 2007; Eisen et al., 2017). To understand tick-borne disease dynamics and what influences host-tick-pathogen interactions, it is essential to understand climatic factors, landscape factors, land use, and human behavior (Pfäffle et al., 2013).

National Ecological Observatory Network

Independent research studies conducted at local scales typically use field sampling approaches that are highly specific for specific questions and hypotheses, and the lack of

standardized sampling methodologies creates challenges for understanding broad-scale patterns (Li et al., 2022). The National Ecological Observatory Network (NEON) was created to address continental-scale questions using standardized methods in a total of 39 terrestrial field sites (excluding Hawaii, Alaska, and Puerto Rico) providing a large scale and long-term open access database, where ecoclimatic variables are studied by 20 ecological regions known as Domains (Paull et al., 2022). These sites are chosen to be representative of ecological and climatological conditions, considering differences in vegetation, landforms, and ecosystem dynamics. NEON's main goal is to be an instrument to understand the interaction between organisms and their environment. The idea of building an observatory network was designed in 1999, developed in 2000, and finally approved in 2011 by the National Science Foundation (NSF), National Science Board, and Congress. NEON began sampling at some sites in the 2010's and became fully operational in 2019. NEON is aiming to collect data freely available for at least 30 years. NEON measurements are directly comparable due to the implementation of standardized methods throughout observations which helps gain a better understanding of ecosystems change and patterns across space and time (Li et al., 2022).

To be able to understand the dynamics of ticks and their pathogens affected by environmental variables, my objectives for my thesis research were to i) characterize the spatiotemporal dynamics of ticks and tick-borne diseases at the local to sub-continental scale across the eastern United States using NEON data; and ii) to relate the abundance of ticks, and the prevalence of tick-borne diseases, to weather variables that are predicted to directly influence tick development and dynamics or indirectly through their effects on seed availability and small mammal host populations.

I focused on the spatial and temporal dynamics of nymph abundance for two species of ticks, *A. americanum* and *I.scapularis*, since they are responsible for the majority of vector-diseases in the United States (Eisen et al., 2017), and on the proportion of infection for these two species. My hypothesis was that tick abundance will be more synchronous at NEON sites close together and that this will be explained by weather variables. I used data obtained from the NEON from a set of Domains from 2014-2021. An understanding of the spatial range and distribution will help with disease detection and prevention on a continental scale. Several factors influencing risk of human exposure to tick-borne diseases have been hypothesized and explained on a local scale, mainly in the Northeast of the United States. Using eight years of data in seven different Domains in the contiguous United States and considering different ecoregions and environmental variables to compare the effects of hypothesized drivers will help gain a better understanding on the interaction in a broader scale. My results provide an understanding of the spatial distribution of ticks and tick-borne disease on a large scale, and in relation to weather cues, which helps scientists understand how environmental changes could determine the risk of tick outbreaks and exposure.

Chapter II - Spatiotemporal dynamics of ticks and tick-borne disease at NEON sites across a sub-continental scale

Introduction

Diseases that are carried by ticks are the primary source of zoonotic pathogens worldwide (Ostfeld et al., 2018), and the family Ixodidae is the most capable of transmitting pathogens to humans (Spach et al., 1993). Lyme disease, which is caused by the bacterium *Borrelia burgdorferi*, is a tick-borne pathogen transmitted through a bite from the Blacklegged tick (*Ixodes scapularis*) (Granter et al., 2014). The alpha-gal allergy, a condition that develops anaphylactic symptoms after ingestion of meat, has increased drastically and is transmitted by the lone star tick (*Amblyomma americanum)* (Jackson, 2018). Changes in temperature may be influencing tick abundance and infection prevalence (Levi et al., 2015) increasing the range of expansion and risks of transmission of tick-borne disease to other species (Karesh et al., 2012).

Patterns of tick abundance and tick-borne disease prevalence at a local scale has been explained through oak reproduction in the northeastern United States and the effect it has on driving the population of seed-eating mammals (e.g., the white-footed mouse (*Peromyscus leucopus*), eastern chipmunk (*Tamias striatus),* and white-tailed deer (*Odocoileus viginianus*) (Elkinton et al., 2004; Janzen, 1971; Ostfeld et al., 2018) that are hosts for ticks (Granter et al., 2014; Ostfeld et al., 2001). The production of seeds (i.e., acorns) by oaks is spatially synchronous and highly variable over time (Granter et al., 2014; Ostfeld et al., 2001; Pearse et al., 2016; Bogdziewicz et al., 2016), and year-to-year fluctuations in these mast-seeding patterns are linked to weather conditions. There is a strong association between weather variables and the production of large seed crops (Sork, 1993). Mast seeding has an indirect effect on tick abundance by increasing the abundance of seed-eating mammals that act as hosts for the ticks. The ΔT method, the difference in temperature between two previous summers ($\Delta T = Temp_{t-1}$ -

$Temp_{t-2}$) has been hypothesized as a cue to predict seed production based on temperature (Kelly et. al., 2013).

Ixodid ticks require three hosts for the completion of a life cycle where they undergo four life stages during their two-year lifespan: egg, larva, nymph, and adult (Eisen et al., 2017; Figure 1). Ticks lay eggs in spring which hatch free of infection into larva during summer months. The nymphal stage is when infection of hosts occurs and is the stage most likely to infect humans (LoGiudice et al., 2003). Temperature influences their life cycle since it may affect host-contact rates and questing tick mortality rates; when warm temperatures are reached, ticks molt into the next stage without delay (Randolph et al., 2002). However, if ticks become active and feed early in the year when temperatures are still low, ticks then have a delay in development leading to diapause (Randolph et al., 2002). Warmer temperatures increase the presence of ticks, leading to higher emergence of zoonotic diseases, and as a result Lyme disease cases in the United States have doubled between 2004 and 2016 (CDC, 2019). Ticks become infected by feeding on an animal host that is carrying the pathogen and molt to become infected nymphs that in turn feed to other hosts, leading to spread of the pathogen transmission (Karasuyama et al., 2020). Tick-borne pathogens are maintained in the zoonotic cycle (Parola & Raoult, 2001).

Understanding spatial patterns of tick dynamics can play a role in determining population density and risk of infection for tick-borne diseases. Drivers of tick population dynamics over a variety of species across larger distances could be explained by potential driving sources such as environmental conditions. Spatially synchronous weather conditions, often referred to as the Moran effect (Moran, 1953), may influence population dynamics across local to regional spatial scales (Liebhold et al., 2004). The Moran effect hypothesizes that sites close together are more

similar in environmental conditions and would be more synchronous than sites farther apart (Ranta et al., 1997). Due to connections between weather and mast seeding (Kelly et al. 2013, LaMontagne et al., 2020, LaMontagne et al., 2021), as well as between mast seeding, small mammals, and ticks (Kelly et al. 2008), spatial patterns in tick population dynamics and the risk of zoonotic outbreaks may potentially be described across broad scales. Following Ostfeld et al. (2006), a model predicting a 2-year-time lag between high seed availability and nymph abundance, the variables that are considered for tick population dynamics are related to weather conditions, particularly July temperature and June precipitation (Ostfeld et al., 2001; Hayes et al., 2015; Figure 1). Even though variables from summer environmental measures need to be taken into account, *I. scapularis* is primarily found in the eastern and central United States and has shown a strong relationship with winter temperature since they show low cold tolerance and overwintering survival (Hayes et al., 2015). However, as *A. americanum* continues to expand its range within the southern and northeastern United States, winter temperatures have little impact on their survival (Whitlow et al., 2021).

Previous research studies are linked to local scales, in the northeastern and north-central United States, where Lyme disease has been a great concern, particularly in regions where deciduous forest are found (Ostfeld et al., 2001, 2006). Tick abundance and tick-borne diseases are influenced by local climate, playing an important role on tick distribution and behavior (Levi et al., 2015; Ostfeld et al., 1995; Randolph et al., 2002). Here, we used tick and tick-borne pathogen data from the National Ecological Observatory Network (NEON) sites spanning 1,735 km for *A. americanum* and 1,477 km for *I. scapularis* across the eastern United States, where ticks are abundant, to fill that gap. NEON collects and provides open access to large-scale and long-term research data using standardized methods (Li et al., 2022). Standardized and repeated

methods over time provides a better understanding of potential drivers of these dynamics that help to understand population variability over long time periods and over large distances. NEON started data collection in 2013 and site locations are thought to be representative of a range of ecological and climatological conditions.

Our objectives for this study were to i) characterize the spatiotemporal dynamics of ticks and tick-borne diseases at the local to sub-continental scale across the eastern United States; and ii) to relate the abundance of ticks, and the prevalence of tick-borne diseases, to weather variables that are predicted to directly influence tick development and dynamics or indirectly through their effects on seed availability and small mammal host populations. We hypothesize that there is a relationship between level of synchrony across sites in tick abundance and in prevalence of tick-borne diseases with distance between sample sites, and that weather variables will influence tick abundance and tick-borne diseases. We predict that nymph abundance for *I. scapularis* will be influenced by January temperature and January precipitation. We also predict that *A. americanum* nymph abundance will be driven by July and June precipitation variables. Moreover, we predict that the proportion of nymphs infected will increase as a result of weather variables that influence small mammal population abundances and climate variables.

Methods

National Ecological Observatory Network (NEON)

We used data obtained from the National Ecological Observatory Network (NEON), an open-access ecological database (www.neoscience.org) which provides large-scale and long-term observation research. NEON contributes to a broader understanding of ecosystem responses through measurements (e.g. terrestrial sampling) in 20 ecoregions, operating three sites within each ecoregion (Kao et al., 2012; Li et al., 2022). The NEON Domains represent distinct regions of ecosystem dynamics with distinct environmental conditions (Paull et al., 2022; Elmendorf &

Thibault, 2020; Li et al., 2022). NEON uses common sampling protocols at all sites and sampling began in some locations in 2010, becoming fully operational across all sites in 2019, and will run for 30 years. There are a total of 39 terrestrial NEON sites excluding Hawaii, Alaska, and Puerto Rico, which are partitioned into 20 ecoclimatic Domains across the United States.

Tick abundance and pathogen prevalence data

At each of the 39 terrestrial NEON sites there are six distributed plots within the NEON sites which are selected randomly for tick sampling, and situated so that the edge of each plot is >150 m from another NEON plot (Elmendorf & Thibault, 2018). Drag sampling consists of dragging a $1m^2$ white flannel cloth around vegetation where the ticks cling and occurs for each of the distributed plots at each site by walking a $160m^2$ perimeter of each of six 40m x 40m tick plots (Elmendorf & Thibault, 2018). A plot must be sampled more than 80 meters to count as a sampled plot, if less than 80 meters are sampled, the sampling is reattempted. Ticks are collected, counted, and categorized by sex and life stage, with data included as the number of ticks per m^2 (Levan et al, 2019). Drag sampling is conducted in different land covers, including multiple forest types (i.e., deciduous forest, mixed forest, and evergreen forest), grassland herbaceous, cultivated crops, pasture hays, and woody wetlands.

We focus on the nymphal stage, because the data available from NEON for nymph was the most comprehensive and the transmission of pathogens to humans is predominantly by the nymphal life stage since adult ticks are large enough to be noted and removed before transmission (Levi et al., 2015). Also, the incidence rate of nymphs carrying a pathogen are likely to be higher in forest land cover and lower within fields (Horobik et al., 2007). We explored the NEON data, and it showed that the number of nymphs were lowest in wetlands and grasslands, and therefore, we only analyzed forest land cover types.

Overall, we focused on NEON tick data products from 13 terrestrial NEON sites that were grouped into seven Domains across the contiguous United States with forest tree cover (Figure 2; Appendix A, Table A1). These sites exceeded a threshold number of tick abundance of greater than three nymphs per site, that excluded NEON sites located in the Pacific Northwest and Southwest from analyses due to the low number of ticks found in these areas; also, human infection with tick-borne pathogens is considered sporadic in the far western United States (Eisen et al., 2017). Ninety-six % of all Lyme disease cases reported to the public health surveillance comes from the 14 states located in the Northeast, mid-Atlantic, and upper Midwest (Eisen et al., 2017). We focus on two species from the Ixodidae family: *A.americanum* and *I. scapularis*. *A. americanum* were found in five NEON Domains and *I. scapularis* were found in four NEON Domains (Figure 2). Overall, the sites that we used in data analyses spanned the eastern United States and distances of up to 1,735 km apart from each other. We used NEON data from 2014-2021 in analyses; due to the COVID-19 pandemic, in 2020 data were not collected at all sites. (As of early May 2023, data from 2022 were still considered provisional, however corrections and extra quality control procedures were still to be done, therefore they were not used in analyses).

For NEON pathogen testing, a target of 130 ticks NEON per site per year (dependent on availability) are selected and sent out to a laboratory for pathogen testing presence or absence (Tsao, 2018). Consequently, not all ticks collected contributed to testing or fewer than 130 nymphs may be used each year. In addition to lacking data in 2020, other site-year combinations may not have data at a NEON site if they did not collect enough nymphal ticks to send for pathogen testing so these were treated as missing data (Sara Paull, NEON Research Scientist, pers. comm.). Nymphs are tested for all possible pathogens depending on species (Tsao, 2018).

The pathogens that were included in the analysis were: *Anaplasma phagocytophilum, Babesia microti, Ehrlichia muris*-like agent, *Borrelia burgdorferi* sensu lato, *Borrelia miyamotoi*, *Borrelia mayonii, Erlichia chaffeensis, Ehrlichia ewingii*, *and Borrelia lonestari* (Table 1). *Amblyomma* species. nymphs were tested for *Francisella tularensis, Rickettsia-rickettsia, Anaplasma phagocytophilum, Erlichia chaffeensis, Ehrlichia ewingii*, *and Borrelia lonestari.* If an individually tested tick was positive for any pathogen, we considered it a positive binary result. *Ixodes* species are targeted for *Anaplasma phagocytophilum, Babesia microti, Ehrlichia muris*-like agent, *Borrelia burgdorferi* sensu lato, *Borrelia miyamotoi* and *Borrelia mayoni*. Note that *Borrelia burgdorferi* and *Borrelia burgdorferi sensu lato* were merged, since the former was an incomplete pathogen name (Li et al., 2022).

Weather data collection

We compiled mean July temperature and total July precipitation data for each NEON plot from ClimateNA, which covers the entire North America (Wang et al., 2016). We used July temperature because according to the tick life stage, larvae molts into nymph during July (Ostfeld et al., 2001; Bouzek et al., 2013). Due to the geographic distribution of *I. scapularis* being mainly located in the Northeast, January precipitation and mean temperature influences overwintering survival. (Hayes et al., 2015). Summer temperature also influences the magnitude of reproduction in many species of trees (Kelly et al., 2013; LaMontagne et al., 2021), and in addition to July temperature, we also used ΔT, the difference in temperature from the two previous summers (July $temp_{t-1}$ - July $temp_{t-2}$) that positively influences the magnitude of seed production by trees (Kelly et al., 2013). In other words, ΔT_3 was calculated using the difference in mean July temperatures in year t-3 and t-4, and ΔT_4 was calculated using the difference in mean July temperatures in year t-4 and t-5, which represents lags in July temperature differences to reflect food for seed-eating small mammal hosts. This high abundance of small mammals

reflected by July temperature of the previous year is when larvae feed and take their first blood meal year t-1; Following questing nymph infecting host in year t which is reflected by July temperature in year t (Figure 1). Due to these time lags, we compiled temperature data for a thirteen-year period, 2009 to 2021.

Analysis

For each tick species separately, we tested for the relationship between the Spearman correlation of synchrony in nymph abundance over time at NEON distributed sampling plots and the spatial distance between NEON plots, and the pairwise Spearman correlation of synchrony in weather variables. To test for these, we ran a multiple regression on these distance matrices using the MRM function in the R package 'ecodist' (Goslee & Urban, 2007). The distance (analyzed as proximity, ranging from 0 to 1) between plots were based on latitude and longitude given their Haversine distance. The models included for spatial synchrony in nymph abundance for *I. scapularis* analysis were: 1. Space including the proximity between plots, 2. Weather reflecting tick-host abundance ($JulyTemp_t$, $JulyTemp_{t-1}$, $JulyTemp_{t-2}$, and $JunePrecip_t$), 2. Lags in July temperature differences to reflect food for seed-eating small mammal hosts (ΔT_3 and ΔT_4), 3. Winter survival ($JanTemp_t$ and $JanPrecip_t$), and 4. A saturated model including all the parameters. The models included for spatial synchrony in nymph abundance for *A. americanum* analysis were: 1. Space including the proximity between plots, 2. Weather reflecting tick-host abundance ($JulyTemp_t$, $JulyTemp_{t-1}$, $JulyTemp_{t-2}$, and $JunePrecip_t$), 2. Lags in July temperature differences to reflect food for seed-eating small mammal hosts (ΔT_3 and ΔT_4), and 4. A saturated model including all the parameters. In addition, we also ran MRM analysis for the pairwise synchrony in the proportion of infected nymphs for each of *I. scapularis* and *A. americanum*; we included: 1. Space including the proximity between plots, 2. Weather reflecting tick-host

abundance ($JulyTemp_t$, $JulyTemp_{t-1}$, $JulyTemp_{t-2}$, and $JunePrecip_t$), 2. Lags in July temperature differences to reflect food for seed-eating small mammal hosts (ΔT_3 and ΔT_4), 3. Nymph abundance in year t, and 4. A saturated model including all the parameters.

We used generalized linear mixed-effects models to test the relationship between environmental factors, nymph abundance during 2014-2021 separately for *I. scapularis, A. americanum*, and pathogen as a binary variable, using glmmTMB package in R (Brooks et al., 2023). To test for the weather variables associated with nymph abundance in *A. americanum* and *I. scapularis*, we conducted the analyses separately for each NEON Domain. These Domains represent separate ecoregion, with different ecosystems dynamics and weather conditions (See appendix, Table A1). For *A. americanum,* the Domains that were included were the Mid-Atlantic Domain, Ozarks Complex Domain, Appalachians & Cumberland Plateau Domain, Southeast Domain, and Prairie Peninsula Domain. For *I. scapularis,* we included Mid-Atlantic, Northeast, Appalachians and Great Lakes. Using Domain-level analyses, we examined tick and tick-borne pathogen relationships with weather, and we then assessed general the patterns in weather drivers for each species. Following Ostfeld et al. (2006), we included terms in the model predicting a 2-year-time lag between high seed availability and nymph abundance. Nymph abundance in year (t) being the year of interest, we included mean July temperature in current year (t), temperature in the previous year (t-1), temperature two years prior (t-2), ΔT_3 (including temperature three years prior (t-3) minus temperature four years prior (t-4)), and ΔT_4(including temperature three years prior (t-4) minus temperature four years prior (t-5)) (Figure 1). Nymphs in year t are affected by small mammals in year t-1, which are driven by mast seeding in year t-2 (Ostfeld et al., 1995). In addition, ΔT has been used to explain the magnitude of reproductive events in trees (Kelly et al., 2013; LaMontagne et al., 2020). ΔT relative to tick abundance was calculated using

the difference in mean July temperatures in year t-3 and t-4 (ΔT_3), and the difference in mean July temperatures in year t-4 and t-5 (ΔT_4). Moreover, January precipitation (in year t) influences nymph population density for the *I. scapularis*, reducing desiccation rates and higher survival (Hayes et al., 2015). As for *A. americanum*, the presence or absence of snow or cold weather had little impact on survival rates, it is a desiccation-tolerant tick having a waxy cuticle preventing water loss, therefore being able to withstand colder temperatures (Whitlow et al., 2021). Temperature variables related to overwintering survival were not included in the models for *A. americanum*. Spring precipitation and forest type were included in the models since high humidity conditions favors tick survival whereas drought conditions and colder winters lead to increased mortality (Ostfeld et al., 2006; Burtis et al., 2016; Schulze et al., 2009).

The proportion of infection in *I. scapularis* and *A. americanum*, has been positively related to temperature and precipitation being the most significant climatic factor related to disease incidence (McCabe & Bunnell, 2004; Pfäffle et al., 2013). Therefore, $JulyTemp_t$, $JulyTemp_{t-1}$, $JulyTemp_{t-2}$, and $JunePrecip_t$ since temperature likely plays a role in survival for every developmental stage, and nymph abundance were included in the models.

Nymph abundance data were treated as a Poisson distribution, and pathogen data were treated as a binomial distribution with zero inflation due to an excess of zeros for the subset for the species *A. americanum*. We tested for zero-inflation using the package DHARMa zero-inflation test, which calculated the expected distribution of zeros against the observed values; a value >1 means that the data has more zeros than expected (Brooks et al., 2017, 2019). In this case, for the proportion of infected nymphs for *A. americanum*, we assumed that infection will mainly vary by environmental factors, therefore we included temperature and precipitation as the zero inflated variables. Therefore, we calculated r2 for models with zero-inflation using

r2_zeroinflated which calculates models with zero-inflation components using the package performance (Lüdecke et al., 2019). The distributed sampling plots at each NEON site were included as random effects in all models.

We used Akaike Information criterion (AICc) to determine the best models for potential drivers of nymph abundance and the proportion of infection in ticks, for each tick species separately, using MuMIn package in R (Barton, K., 2020). We specified a global model including predictor variables based on the terms presented above for *I. scapularis* (Land cover type, ΔT_3, ΔT_4, $JunePrecip_t$,$JulyTemp_t$, $JulyTemp_{t-1}$, $JulyTemp_{t-2}$, $JanTemp_t$, and $JanPrecip_t$) and *A. americanum* nymph abundance (Land cover type, ΔT_3, ΔT_4, $JunePrecip_t$, $JulyTemp_t$, $JulyTemp_{t-1}$, and $JulyTemp_{t-2}$) and for the proportion of nymph infected ($JunePrecip_t$,$JulyTemp_t$, $JulyTemp_{t-1}$, and $JulyTemp_{t-2}$). We determined the best model set based on ΔAIC_c (<2) and AIC_c weights. AICc was used to compare different possible models and determine which single model or set of models is the best for the data (Burnham and Anderson, 2004). We used R version 4.1.2 for all statistical analyses.

Results

Nymph population trends

We found that the mean of nymph abundance (# ticks/m^2) across years for the NEON sampling plots showed a high variability over time and space, with a mean population coefficient of variation for *A. americanum* across the NEON distributed sampling plots of 1.25 ± 10.7 (minimum CV = 0.12, maximum CV = 9.38); and for the *I. scapularis* the coefficient of variation was 0.87 ± 2.97(minimum CV = 0.29, maximum CV = 3.61) (Appendix Figure A1).

Spatial patterns of nymph abundance

For both species, *A. americanum* and *I. scapularis*, spatial synchrony declined significantly with increasing distances between NEON plots (Figure 2). In the MRM analysis, spatial synchrony of nymph abundance for *A. americanum* was significantly explained by proximity between the

distributed sampling plots (P = 0.001), and by the model including spatial synchrony in ΔT_3 and ΔT_4 (P = 0.025). In the saturated model, proximity and ΔT_3 and ΔT_4 also significantly explained spatial synchrony in nymph abundance (Table 2 and Figure 4). For *I. scapularis*, patterns of synchrony in nymph abundance were significantly explained by proximity between the distributed sampling plots, with a negative relationship between synchrony and the increased distance between plots (P = 0.005) and by the model including synchrony in January temperature and precipitation between sites (P = 0.042). However, for *I. scapularis* the saturated model did not significantly explain patterns of spatial synchrony (Table 3 and Figure 5).

Proportion of nymph infected

The ecological variables that were significant in models of spatial synchrony in the MRM analysis for the proportion of *A. americanum* nymphs infected with a pathogen included nymph abundance (P = 0.010) (Table 4 and Figure 6). The saturated model included nymph abundance and $JulyTemp_{t-1}$ as significant variables. Conversely, spatial synchrony for the proportion of *I. scapularis* nymphs carrying a pathogen was not significantly explained by proximity (it did not significantly change with an increased distance between plots). Moreover, when analyzing the weather variables explaining the proportion of *I. scapularis* nymphs infected with a pathogen, none of the variables present in the MRM analysis were significant (see Appendix Table A2 and Figure A2).

We looked at the Spearman correlations between *I. scapularis* and *A. americanum* for seven sites where both species overlapped. We considered a minimum of three years of overlap in the time series and excluded the sites that had only one tick sampled in total, therefore three sites were excluded (LENO (Ozarks Complex Domain), TALL (Ozarks Complex Domain), and UKFS (Prairie Peninsula Domain). Spearman correlation analyses demonstrated that there is a non-significant but positive correlation between the tick species in the Mid-Atlantic Domain:

BLAN (r=0.46 and p-value=0.30), SCBI (r=0.69 and p-value=0.06), and SERC(r=0.14 and p-value=0.78) and a negative but non-significant correlation between the two species in the Appalachians: ORNL (r=-0.59 and p-value=0.13), (Figure A3, see Appendix Table A3).

Weather predictors for nymph abundance

To determine the best model(s) that were combinations of weather predictors for patterns in nymph abundance for *A. americanum* and *I. scapularis*, the analyses were conducted separately for each NEON Domain.

A. americanum

The results of the weather variables in models for *A. americanum* nymph abundance were highly consistent throughout NEON Domains. *A. americanum* nymph abundance over time in the Mid-Atlantic Domain was best predicted by a model with a positive effecs in ΔT_3, ΔT_4, and $JulyTemp_{t-1}$ (AICc weight = 0.197, conditional R2 (cR^2) = 0.738, Table 5 and Appendix Figure A4 part A), which was followed by three other models within $\Delta AICc < 2$ were the more common variables present in these models were ΔT_3, ΔT_4, $JulyTemp_{t-1}$ and $JulyTemp_{t-2}$. In the Southeast Domain, a positive effect of ΔT_3 (the difference of $JulyTemp_{t-3}$ and $JulyTemp_{t-4}$) which corresponds to the two summers prior to a mast event, was the best to explain nymph abundance for *A. americanum* (AICc weight = 0.318 and $cR^2 = 0.736$, Table 5 and Appendix Figure A4 part A). For the Appalachians & Cumberland Plateau Domain, the top model included a positive effect of ΔT_4 and negative effect of $JunePrecip_t$ (AICc weight = 0.226 and $cR^2 = 0.899$, Table 5 and Appendix Figure A4 part B), followed by a second model ($\Delta AICc = 1.25$) that included a positive effect ΔT_4, negative effect of $JunePrecip_t$, and negative effect of $JulyTemp_t$. *A. americanum* nymph abundance for Ozarks Complex Domain was driven by negative effect ΔT_3, a positive effect of ΔT_4, a positive effect of land cover type, a positive effect of $JunePrecip_t$, a positive effect of $JulyTemp_{t-2}$, and a positive effect of $JulyTemp_t$ (AICc weight = 0.676, cR^2 =

0.912, Table 5 and Appendix Figure A4 part C). In the Prairie Peninsula Domain, the top model for nymph abundance included a negative effect of ΔT_4, a positive effect of $JunePrecip_t$, and positive effect of $JulyTemp_{t-1}$ (AICc weight = 0.134, cR^2=0.772, Table 5).

I. scapularis

In the Northeast Domain, the top variables in models of *I. scapularis* nymph abundance included a negative effect of $JanTemp_t$ and negative effect of $JunePrecip_t$ (AICc weight = 0.037, Table 6 Appendix Figure A5 part A). This model was followed by positive effect of ΔT_3 and negative effect of $JanTemp_t$ (ΔAICc = 0.43), and by a model with only negative effect of $JanTemp_t$ (ΔAICc = 0.51). Overall, there were six more models also included in the set of models ΔAICc of <2, all included temperature and precipitation variables. Consistent with the Northeast Domain, the Great Lakes Domain also showed that nymph abundance drivers were related to temperature and precipitation, however the top model included negative effect of ΔT_4, a negative effect of $JunePrecip_t$, a negative effect of $JulyTemp_{t-1}$, and a positive effect $JulyTemp_t$ (AICc weight = 0.115, cR^2 = 0.762, Table 6 and Appendix Figure A5 part A) followed by two other models including ΔT_3, ΔT_4, $JunePrecip_t$, $JulyTemp_{t-2}$, and $JulyTemp_t$; and ΔT_3, ΔT_4, $JunePrecip_t$, $JulyTemp_{t-1}$, and $JulyTemp_t$ (ΔAICc = 0.19 and 1.81, respectively, Table 6 and Appendix Figure A5 part A). The dynamics of *I. scapularis* populations sampled in the Mid-Atlantic Domain were best described as a response of a model with the terms a negative effect of ΔT_3, a positive effect of ΔT_4, a positive effect $JanPrecip_t$, a positive effect of $JanTemp_t$, and a positive effect of $JulyTemp_{t-1}$ (AICc weight= 0.115 and cR^2=0.824, Table 6 and Appendix Figure A5 part A). Followed by two other models, including ΔT_3, ΔT_4, $JanTemp_t$, and $JulyTemp_{t-1}$ (omitting $JanPrecip_t$ from the top model) and ΔT_3, ΔT_4, JanPrecip, $JanTemp_t$, $JunePrecip_t$, and $JulyTemp_{t-1}$ (which added $JunePrecip_t$ into the top model; ΔAICc = 0.070 and 0.044, respectively, Table 6).

For the Appalachians & Cumberland Plateau Domain, the null model was the best model (with an AICc weight = 0.100, Table 6 and Appendix Figure A5 part B) and followed by three models also included in the set of models ΔAICc of <2, including one weather variable each, either ΔT_3, ΔT_4, or $JulyTemp_{t-1}$ (ΔAICc = 0.43, 1.82, and 1.94, respectively, Table 6).

Predictors of the proportion of infected ticks

A. americanum

The proportion of infected *A. americanum* nymphs in the Mid-Atlantic Domain was explained by the top zero-inflated model (zero-inflated terms are indicated with 'zi') of a negative effect of $JunePrecip_t$, a negative effect of $JulyTemp_{t-1}$, a positive effect of $JulyTemp_{t-2}$, a negative effect of zi ($JunePrecip_t$), a negative effect of zi ($JulyTemp_{t-1}$), and a positive effect of zi ($JulyTemp_t$), AICc weight = 0.109 (Table 7). There were 13 additional models present with a ΔAICc < 2. The most common variables in these additional models were $JunePrecip_t$, $JulyTemp_{t-1}$, $JulyTemp_{t-2}$, zi ($JunePrecip_t$), zi ($JulyTemp_t$), and $JulyTemp_{t-2}$. In the Southeast Domain, a negative effect of zi ($JulyTemp_{t-1}$) was the main driver of the proportion of infected *A. americanum* ticks (AICc weight=0.32, Table 7). This was similar in the Prairie Peninsula Domain with the top model being $JunePrecip_t$ with a positive effect and zi ($Julytemp_{t-1}$) with a positive effect (AICc weight = 0.199) and followed by a model with only $JunePrecip_t$ with a positive effect (ΔAICc = 0.80). For the Appalachians & Cumberland Plateau Domain the top included a negative effect of $JunePrecip_t$, a negative effect $JulyTemp_{t-2}$, a negative effect zi ($JulyTemp_{t-1}$), a positive effect zi ($JulyTemp_t$) (AICc weight = 0.167, Table 7). The next best model was similar to the top model, replacing the term a negative effect $JulyTemp_{t-2}$ with a negative effect $JulyTemp_{t-1}$ (ΔAIC_c = 0.97) and followed by three other models with ΔAICc <2 with zi ($JulyTemp_{t-1}$) and zi ($JulyTemp_t$) being the most common variables. Finally, a negative effect of zi ($JulyTemp_{t-1}$) was the top model to explain nymph abundance in the Ozarks Complex Domain (AIC weight=

0.170), followed by other two models where zi ($JulyTemp_{t-1}$) was the most common variables (ΔAICc = 1.20 and 1.56, respectively).

I. scapularis

The top model for the proportion of *I. scapularis* nymphs infected with a pathogen in the Northeast Domain included a negative effect of $JulyTemp_{t-1}$ and a negative effect of $JulyTemp_{t-2}$ (AICc weight = 0.216, Table 8) and followed by three other models with ΔAICc < 2, a model with only the variable $JulyTemp_{t-1}$, the null model, and a model with $JulyTemp_{t-1}$ and $JulyTemp_t$ (Table 8). The Mid-Atlantic Domain showed a positive effect $JulyTemp_t$ (AICc weight=0.371, Table 8) being the top model, followed by a model with $JulyTemp_{t-2}$ and $JulyTemp_t$ (ΔAICc= 1.30, Table 8). For both the Great Lakes Domain and Appalachians & Cumberland Plateau Domain, they had the null model as the top model (AICc weights = 0.220 and 0.314, respectively, Table 8).

Discussion

Our results showed that there is a relationship between the level of synchrony in tick abundance and distance across sites. Spatial synchrony declined significantly with increasing distances between NEON sampling plots for both *Amblyomma americanum* and *Ixodes scapularis* nymph abundance, supporting our hypothesis of a relationship between levels of synchrony with distance. We found that some of weather variables that were consistent throughout the models for synchrony in tick abundance between sampling plots and the magnitude of tick abundance at plots for *A. americanum* were related to ΔT_3 and ΔT_4, which tended to show positive effects on nymph abundance. For *I. scapularis,* overwintering survival was determined by the coldest month. A negative effect of January temperature and positive effect of January precipitation were the most common variables present in the analyses for AICc and were significantly explained by

the MRM. A negative effect of June precipitation of year t and a positive effect of July temperature of the previous year were the most common variables present in the models of the prevalence of infection *A. americanum*. However, the spatial synchrony in the proportion of infection of *A. americanum* was explained by nymph abundance in year t. For *I. scapularis* and *A. americanum* nymph abundance, the results supported our hypotheses of a relationship between level of synchrony in nymph abundance and weather variables. However, for the prevalence of infection of *A. americanum* we rejected the hypothesis that there was relationships between synchrony across sampling plots with distance, and we supported our hypothesis that weather variables have an influence in tick abundance and tick-borne diseases. The proportion of infection of *I. scapularis* ticks was not significantly explained by the variables we used, therefore we reject both hypotheses for this species. The patterns across domains for both species nymph abundance were consistent, with some exceptions in the Great Lakes Domain and Appalachians and Cumberland Plateau Domain for *I. scapularis* nymph abundance.

Spatial patterns of nymph abundance

Synchrony in the dynamics of *A. americanum* nymph abundance was explained by plot proximity (closer plots were more synchronous), ΔT_3 and ΔT_4, with ΔT, being cues related to seed availability (Kelly et al., 2013) that influences host abundance. Nymph abundance for *I. scapularis* has been hypothesized to be influenced by mast seeding, due to the availability of hosts (Borgmann-Winter et al., 2021), and mast seeding is associated with an increased abundance of questing nymphs (Ostfeld et al., 2018). Mid-Atlantic Domain, Southeast Domain, Appalachiand & Cumberland Plateau showed a positive effect of ΔT_3 and ΔT_4..However, for some domains including Prairie Peninsula Domain and Ozarks Complex Domain for *A. americanum*, and for Great Lakes and Mid-Atlantic for *I. scapularis*, there was a negative effect of ΔT_3 and ΔT_4. It has been discussed that mast seeding increases the abundance of rodents and

the presence of this later could increase the presence of predators of rodents, that are then associated with the reduction of nymphs (Ostfeld et al., 2018).

Ticks spend the large majority of their life cycle off-hosts, and therefore ticks are directly influenced by seasonal and daily environmental conditions (Mangan et al., 2018). There has been a lack of agreement in what weather variables influence nymph abundance. Solely summer temperatures (July and June precipitation) have been used (Hayes et al., 2015; Ostfeld et al., 2006), however, the ability to overwinter plays an important role in nymph survival for some species in some locations (Hayes et al., 2015; Whitlow et al., 2021). Spatial synchrony in *I. scapularis* population dynamics in our study was explained by proximity between plots and spatial synchrony in temperature in the coldest month, January. Our findings support Hayes et al. (2015) hypothesis that overwintering survival for *I. scapularis* is a main driver to understand annual nymph abundance; and that January temperature and precipitation explains spatial synchrony of this species. For *I. scapularis* nymph abundance in year t, we found that for the Northeast Domain and the Mid-Atlantic Domain that January temperature was one of the drivers, accompanied with June Precipitation. Although in the Great Lakes Domain we expect cold winters, winter temperature was not included in the model June Precipitation and July temperature were the most common variable.

Increased precipitation has a positive effect on breaking larval diapause which increases success in nymphal questing survival (McCabe & Bunnell, 2004). Soil moisture due to rainfall in forested areas favors tick survival (McCabe & Bunnell, 2004), however, our results indicated that June precipitation had a negative effect in *I. scapularis* and *A. americanum* nymph abundance. It is important to note that the focus of previous research has been largely isolated the northeastern region of the United States (Burtis et al., 2016; McCabe & Bunnell, 2004;

Ostfeld et al., 2001; Schulze et al., 2009) and we examined a much broader geographic range. This negative effect on a broader scale could be due to changes in water retention due to climate change. Global warming has disrupted hydrological effects by increasing evaporation rate of water in some areas leading to droughts and other areas are experiencing extreme precipitation events (Asif et al., 2023). Flooding and drought influence tick abundance, most of the tick eggs die during these dramatic events.

Predictors of proportion of nymph infected

We found that the proportion of infection *A. americanum* was driven by June precipitation of year t and July temperature of the previous year, which was consistent across Domains. Therefore, this indicates that the temperature driving the hosts of ticks plays a role in the proportion of ticks carrying an infection. High humidity enhances tick survival, favoring conditions of infection (McCabe & Bunnell, 2004). We found that the overall spatial synchrony in the proportion *A. americanum* specimens infected with a pathogen across all NEON sampling plots was best explained by synchrony in nymph abundance in the year t. The proportion of infected ticks' spatial synchrony for the species *A. americanum* was significantly explained by nymph abundance. Our results could not show that the proportion of infection and nymph abundance are synchronous since there is high variability across sampling plots. Therefore, we cannot predict if there will be more of fewer infected nymphs in a local site.

We were unable to detect the drivers of the spatial synchrony in the proportion of infected individuals for *I. scapularis*, with no model being statistically significant. *I. scapularis* has had a reduction of density of questing nymphs in areas within a long-term endemic region when temperatures increase, therefore environmental variables could have been masked in recently endemic areas (Burtis et al., 2016).

Limitations and future research

Limitations of the current study is that our analyses were based on the assumption that environmental variables could explain host availability, based on Holland et al. (2015). We assumed that the mean temperature and total precipitation for July (including time lags), and January temperature were accurate proxy measurements to explain nymph abundance and tick-borne disease prevalence. Similarly, we assumed that nymph mean abundance for *A. americanum* and *I. scapularis* per distributed sampling plot per year corresponding to a NEON Domain/ecoregion was representative of the ecoregion. There is no previous literature using model comparison approach testing for interaction of *A. americanum*, their host, and their responses to tree reproduction. Therefore, for this research since *I. scapularis* and *A. americanum* share the same life cycle we assumed that *A. americanum* could be correlated with prior abundance of host and food resources for those hosts, explained by weather cues. Most of the literature is focused in the Northeast United States and the species *I. scapularis* (Ostfeld et al., 1995, 2006, 2018; LoGiudice et al., 2003; Granter et al., 2014), which formed a basis for much of our approach. Tick abundance and tick-borne disease prevalence at a local scale have been explained through oak reproduction in the northeastern United States (Granter et al., 2014; Ostfeld et al., 2001; Pearse et al., 2016), however it has not been understood nor explained at a broader subcontinental scale.

In this study, we characterized the spatiotemporal dynamics of ticks and tick-borne diseases at the local to sub-continental scale across the eastern United States, and we related the abundance in ticks and tick-borne diseases to climate data. Future research could address host availability with using small mammal data since host abundance may be more important than weather patterns to discuss infection proportion since it causes nymphal dispersion, therefore a higher proportion of infection. As more NEON data are collected, this could be pursued.

Likewise, future studies could include mast seeding data, however NEON does not collect mast seeding data. Also, ticks have expanded geographic range northwards due to climatic warming (Gray & Ogden, 2021; Levi et al., 2015) and likely affects tick population dynamics. Climate change favors the faster development of ticks due to milder winters and higher average temperatures (Pfäffle et al., 2013), causing larvae to molt into nymphs earlier since ticks are highly sensitive to temperature and moisture in their off-host phase (Ledger et al., 2019) and they may therefore complete a life cycle in less than two years. This research is a steppingstone to understanding tick dynamics and tick distribution on a sub-continental scale and may lead to improved predictions for future tick-borne diseases outbreaks.

Tables and Figures

Table 1. Tick pathogens in *I. scapularis* and *A. americanum* used from NEON.

Disease	**Primary vector(s)**	**Etiological agent(s)**
Anaplasmosis	*Ixodes scapularis*	*Anaplasma phagocytophilum*
Babesiosis	*Ixodes scapularis*	*Babesia microti*
Borrelia miyamotoi disease	*Ixodes scapularis*	*Borrelia miyamotoi*
Ehrlichiosis	*Ixodes scapularis*	*Ehrlichia muris*
	Amblyomma americanum	*Ehrlichia ewingii*
	Amblyomma americanum	*Ehrlichia chaffeensis*
Lyme disease	*Ixodes scapularis*	*Borrelia burgdorferi*
	Ixodes scapularis	*Borrelia mayonii*
Southern Tick-Associated Rash Illness	*Amblyomma americanum*	*Borrelia lonestari*

Table 2. Multiple regression on distance matrices (MRM) results for proximity and weather factors influencing the mean synchrony of *A. americanum* in year t.

Model & Variables	Coefficient	P (variable)	R^2 (model)	P (model)
1. Space			0.0020	**0.001**
Proximity	0.004	**0.001**		
2. Weather: Host variables			0.0003	0.736
$JulyTemp_t$	0.005	0.752		
$JunePrecip_t$	-0.022	0.117		
$JulyTemp_{t-1}$	-0.018	0.368		
$JulyTemp_{t-2}$	0.002	0.230		
3. Mast seeding variables			0.0015	**0.025**
ΔT_3	-0.196	**0.026**		
ΔT_4	0.215	**0.008**		
4. Saturated model			0.0041	**0.031**
Proximity	0.067	**0.001**		
$JulyTemp_t$	-0.012	0.531		
$JunePrecip_t$	-0.008	0.703		
$JulyTemp_{t-1}$	-0.018	0.424		
$JulyTemp_{t-2}$	-0.005	0.817		
ΔT_3	-0.205	**0.012**		
ΔT_4	0.209	0.013		

Table 3. Multiple regression on distance matrices (MRM) results for proximity and weather factors influencing the mean synchrony of *I. scapularis* in year t.

Model & Variables	Coefficient	P (variable)	R^2 (model)	P (model)
1. Space			**0.0010**	**0.005**
Proximity	-0.005	**0.011**		
2. Weather: Host variables			0.0002	0.831
$JulyTemp_t$	-0.005	0.663		
$JunePrecip_t$	0.009	0.425		
$JulyTemp_{t-1}$	-0.025	0.362		
$JulyTemp_{t-2}$	0.021	0.432		
3. Winter survival			0.0009	**0.042**
$JanTemp_t$	0.015	0.132		
$JanPrecip_t$	0.023	0.660		
4. Mast seeding variables			0.0008	0.750
ΔT_3	0.022	0.373		
ΔT_4	-0.025	0.404		
5. Saturated model			0.0014	0.258
Proximity	0.029	**0.035**		
$JulyTemp_t$	-0.005	0.673		
$JunePrecip_t$	-0.010	0.334		
$JanTemp_t$	0.030	0.133		
$JanPrecip_t$	0.021	0.159		
$JulyTemp_{t-1}$	-0.017	0.548		
$JulyTemp_{t-2}$	0.006	0.844		
ΔT_{3-4}	0.024	0.409		
ΔT_{4-5}	-0.021	0.453		

Table 4. Multiple regression on distance matrices (MRM) results for proximity, weather factors, and *A. americanum* nymph abundance influencing the proportion of synchrony of infected ticks in year t.

Model & Variables	Coefficient	P (variable)	R^2 (model)	P (model)
1. Space			0.003	0.849
Proximity	-0.006	0.849		
2. Weather: Host variables			0.007	0.092
$JulyTemp_t$	0.004	0.895		
$JunePrecip_t$	0.005	0.506		
$JulyTemp_{t-1}$	0.113	0.012		
$JulyTemp_{t-2}$	-0.104	0.033		
3. Nymph abundance			0.276	**0.010**
Nymphs	0.525	**0.001**		
4. Mast seeding variables			0.005	0.641
ΔT_3	-0.078	0.639		
ΔT_4	0.059	0.710		
5. Saturated model			0.013	**0.001**
Proximity	0.039	0.543		
$JulyTemp_t$	0.007	0.807		
June Precipitation	-0.003	0.943		
Nymphs	0.067	**0.015**		
$JulyTemp_{t-1}$	0.118	**0.011**		
$JulyTemp_{t-2}$	-0.088	0.075		
ΔT_3	-0.117	0.722		
ΔT_4	-0.003	0.943		

Table 5. Summary of ΔAICc values <2 for generalized linear mixed effects models of *A. americanum* nymph abundance per Domain. Including predictor variables field type, ΔT_3, ΔT_4, Mean July Temperature, mean July temperature of previous year, mean July temperature of two previous years, and June precipitation, using plots ID as a random effect, from 2014 to 2021.

Model Terms	LL	K	ΔAICc	W_i	cR^2	mR^2
D02-Mid-Atlantic						
ΔT_3+ ΔT_4+$JulyTemp_{t-1}$	-210.9	5	0.00	0.197	0.738	0.325
ΔT_3+ ΔT_4+$JulyTemp_{t-1}$+$JulyTemp_t$	-210.5	6	1.48	0.094	0.757	0.357
ΔT_3+ ΔT_4+$JulyTemp_{t-1}$+$JulyTemp_{t-2}$	-210.6	6	1.56	0.090	0.721	0.299
ΔT_3+ ΔT_4+$JulyTemp_{t-2}$+$JulyTemp_t$	-210.7	6	1.81	0.079	0.757	0.357
D03-Southeast						
ΔT_3	-35.97	3	0.00	0.318	0.736	0.104
D06- Prairie Peninsula						
ΔT_4 + $JunePrecip_t$+ $JulyTemp_{t-1}$	-170.21	5	0.00	0.134	0.772	0.296
ΔT_4	-173.32	3	0.94	0.084	0.737	0.236
ΔT_4+ $JulyTemp_{t-1}$	-172.14	4	1.13	0.076	0.752	0.263
ΔT_3 +ΔT_4 +$JulyTemp_{t-1}$	-170.86	5	1.32	0.069	0.761	0.286
ΔT_3 +ΔT_4	-172.34	4	1.55	0.062	0.743	0.253
ΔT_4 +$JulyTemp_t$	-172.35	4	1.56	0.062	0.764	0.278
ΔT_4+ $JulyTemp_{t-1}$+ $JulyTemp_{t-2}$	-171.32	5	1.91	0.052	0.759	0.287
D07- Appalachians & Cumberland Plateau						
ΔT_4+$JunePrecip_t$	-165.14	4	0.00	0.226	0.899	0.405
ΔT_4+$JunePrecip_t$+ $JulyTemp_t$	-164.52	5	1.25	0.121	0.897	0.410
D08-Ozarks Complex						
ΔT_3 +ΔT_4 +$JunePrecip_t$ +$JulyTemp_{t-2}$+ $JulyTemp_t$ +Forest type	-179.78	9	0.00	0.676	0.912	0.631

Table 6. Summary of ΔAICc values <2 for generalized linear mixed effects models of *I. scapularis* nymph abundance per Domain. Including predictor variables field type, ΔT_3, ΔT_4, July Temperature, July temperature of previous year, July temperature of two previous years,January temperature, January precipitation, and June precipitation, using plots ID as a random effect, from 2014 to 2021.

Model Terms	LL	K	ΔAICc	W_i	cR^2*	mR^2
D01-Northeast						
$JanTemp_t$+$JunePrecip_t$	-83.82	4	0.00	0.037	0.288	0.164
$JanTemp_t$ +ΔT_3	-84.04	4	0.43	0.030	0.259	0.134
$JanTemp_t$	-85.29	3	0.51	0.029	0.227	0.100
$JanPrecip_t$+$JunePrecip_t$+$JulyTemp_t$ +$JulyTemp_{t-2}$	-81.50	6	0.64	0.027	0.347	0.231
$JanTemp_t$+ $JunePrecip_t$+ $JulyTemp_t$	-83.07	5	1.07	0.022	0.307	0.199
$JanTemp_t$ +ΔT_3 + $JunePrecip_t$+ $JulyTemp_t$	-83.08	5	1.09	0.022	0.317	0.203
$JunePrecip_t$ +$JulyTemp_t$+ $JulyTemp_{t-2}$	-83.43	5	1.78	0.015	0.297	0.171
$JanTemp_t$+ $JulyTemp_{t-1}$	-84.76	4	1.88	0.015	0.244	0.133
$JanPrecip_t$+$JulyTemp_{t-1}$+ $JulyTemp_{t-2}$	-83.51	5	1.95	0.014	0.264	0.146
D02- Mid-Atlantic						
$JanTemp_t$+ΔT_3+ ΔT_4+$JanPrecip_t$+$JulyTemp_{t-1}$	-206.22	7	0.00	0.115	0.824	0.330
$JanTemp_t$+ΔT_3+ ΔT_4+$JulyTemp_{t-1}$	-207.92	6	1.00	0.070	0.830	0.323
$JanTemp_t$+ΔT_3+ ΔT_4+$JanPrecip_t$ + $JunePrecip_t$+$JulyTemp_{t-1}$	-205.97	8	1.94	0.044	0.818	0.322
D05-Great Lakes						
$JunePrecip_t$ +ΔT_4+ $JulyTemp_t$ +$JulyTemp_{t-1}$	-109.57	6	0.00	0.215	0.762	0.328
$JunePrecip_t$ +ΔT_3+ ΔT_4+ $JulyTemp_t$ +$JulyTemp_{t-2}$	-108.29	7	0.19	0.196	0.796	0.316
$JunePrecip_t$ +ΔT_3+ ΔT_4 + $JulyTemp_t$+$JulyTemp_{t-1}$	-109.09	7	1.81	0.087	0.764	0.333

D07- Appalachians & Cumberland Plateau						
Null model	-59.91	2	0.00	0.100	NA	0.000
ΔT_4	-58.97	3	0.43	0.080	NA	0.054
ΔT_3	-59.66	3	1.82	0.040	NA	0.015
$JulyTemp_{t-1}$	-59.72	3	1.94	0.038	NA	0.011

*NA for D07 because random effect of distributed plot were not able to be processed in this model.

Table 7. Summary of ΔAICc values <2 for zero-inflated mixed effects models of proportion of *A. americanum* nymphs infected with a pathogen (binomial distribution), analyzed for each Domain. Tested models included mean July Temperature, mean July temperature of previous year, mean July temperature of two previous years, and June precipitation, as well as these terms as zero-inflated predictors, with plot ID as a random effect, from 2014 to 2021.

Model Terms	LL	K	ΔAICc	W_i	mR^2
D02-Mid-Atlantic					
$JunePrecip_t$+ $JulyTemp_{t-1}$+ $JulyTemp_{t-2}$+ zi ($JunePrecip_t$) + zi($JulyTemp_{t-1}$) + zi($JulyTemp_t$)	-17.65	8	0.00	0.109	0.456
$JulyTemp_{t-1}$+ $JulyTemp_t$ + zi ($JunePrecip_t$) + zi($JulyTemp_{t-1}$)	-19.16	7	0.24	0.096	0.453
$JulyTemp_{t-2}$ + zi ($JulyTemp_{t-1}$) + zi($JulyTemp_{t-2}$) + zi($JulyTemp_t$)	-19.44	7	0.81	0.073	0.116
$JunePrecip_t$+ $JulyTemp_{t-1}$+ zi ($JunePrecip_t$) + zi($JulyTemp_t$)	-19.56	7	1.06	0.064	0.316
$JunePrecip_t$+ $JulyTemp_{t-1}$+ $JulyTemp_{t-}$ + zi($JunePrecip_t$) + zi($JulyTemp_t$)	-18.19	8	1.09	0.063	0.589
$JulyTemp_{t-1}$	-23.48	4	1.27	0.057	0.114
$JulyTemp_{t-1}$+ $JulyTemp_t$+ zi($JunePrecip_t$)	-21.02	6	1.31	0.056	0.453
$JunePrecip_t$ + $JulyTemp_{t-1}$+ $JulyTemp_{t-2}$ + $JulyTemp_t$ + zi($JunePrecip_t$) + zi($JulyTemp_t$)	-16.88	9	1.31	0.056	0.776
zi($JulyTemp_{t-2}$)	-23.53	4	1.38	0.055	0.000
$Julytemp_{t-1}$+ zi($JunePrecip_t$) + zi($JulyTemp_{t-1}$) + zi($JulyTemp_{t-2}$)	-19.73	7	1.39	0.054	0.175
$JunePrecip_t$+ $JulyTemp_{t-2}$ + zi($JulyTemp_{t-1}$) + zi($JulyTemp_{t-2}$)	-19.75	7	1.42	0.053	0.136
$JulyTemp_{t-1}$+ $JulyTemp_t$+ zi($JunePrecip_t$) + zi($JulyTemp_t$)	-19.79	7	1.52	0.050	0.406
$JulyTemp_{t-1}$+ zi($JunePrecip_t$) + zi($JulyTemp_t$)	-21.14	6	1.57	0.049	0.132
$JunePrecip_t$ + $JulyTemp_{t-2}$+ $JulyTemp_t$ + zi($JulyTemp_{t-1}$) + zi($JulyTemp_{t-2}$)	-18.47	8	1.64	0.048	0.297

D03-Southeast					
zi($JulyTemp_{t-1}$)	-19.87	4	0.00	0.32	0.000
D06-Prairie Peninsula					
$JunePrecip_t$+ zi($JulyTemp_{t-1}$)	-38.89	5	0.00	0.199	0.112
$JunePrecip_t$	-40.55	4	0.80	0.134	0.088
D07- Appalachians & Cumberland Plateau					
$JunePrecip_t$+ $JulyTemp_{t-2}$+ zi($JulyTemp_{t-1}$) + zi($JulyTemp_t$)	-24.11	7	0.00	0.167	0.234
$JunePrecip_t$ + $JulyTemp_{t-1}$+ zi($JulyTemp_{t-1}$) + zi($JulyTemp_t$)	-24.60	7	0.97	0.102	0.123
zi($JulyTemp_{t-1}$)	-29.18	4	1.42	0.082	0.000
zi($JulyTemp_t$)	-27.94	5	1.66	0.073	0.000
$JunePrecip_t$ + $JulyTemp_{t-1}$+ zi($JunePrecip_t$) + zi($JulyTemp_{t-1}$)+ zi($JulyTemp_t$)	-23.36	8	1.83	0.066	0.055
D08-Ozarks Complex					
zi($JulyTemp_{t-1}$)	-6.43	4	0.00	0.170	0.000
$JulyTemp_{t-1}$ + zi($JulyTemp_{t-1}$)	-5.68	5	1.20	0.095	0.663
$JulyTemp_{t-2}$ + zi($JulyTemp_{t-1}$)	-5.87	5	1.56	0.079	0.153

Table 8. Summary of ΔAICc values <2 for generalized linear mixed effects models of *I. scapularis* nymphs infected with a pathogen (binomial distribution), analyzed for each Domain. Predictors include mean July Temperature, mean July temperature of previous year, mean July temperature of two previous years, and June precipitation, using plots ID as a random effect, from 2014 to 2021.

Model Terms	LL	K	ΔAICc	W_i	cR^2	mR^2
D01-Northeast						
$JulyTemp_{t-1}$+$JulyTemp_{t-2}$	-35.41	4	0.00	0.216	0.062	0.062
$JulyTemp_{t-1}$	-36.95	3	0.47	0.171	0.026	0.026
Null model	-38.52	2	1.21	0.118	0.000	0.000
$JulyTemp_{t-1}$+ $JulyTemp_t$	-36.32	4	1.81	0.087	0.055	0.055
D02-Mid-Atlantic						
$JulyTemp_t$	-58.14	3	0.00	0.371	0.080	0.080
$JulyTemp_{t-2}$ + $JulyTemp_t$	-57.56	4	1.30	0.193	0.079	0.079
D05-Great Lakes						
Null model	-42.63	2	0.00	0.220	0.000	0.000
$JulyTemp_t$	-41.54	3	0.34	0.185	0.014	0.14
$JulyTemp_{t-1}$	-42.14	3	1.54	0.102	0.034	0.009
$JulyTemp_{t-1}$+ $JulyTemp_t$	-40.97	4	1.94	0.083	0.030	0.030
D07-Appalachians & Cumberland Plateau						
Null model	-6.28	2	0.00	0.314	0.000	0.000
$JulyTemp_{t-2}$	-5.65	3	1.72	0.133	0.099	0.099
$JulyTemp_t$	-5.79	3	1.99	0.116	0.067	0.067

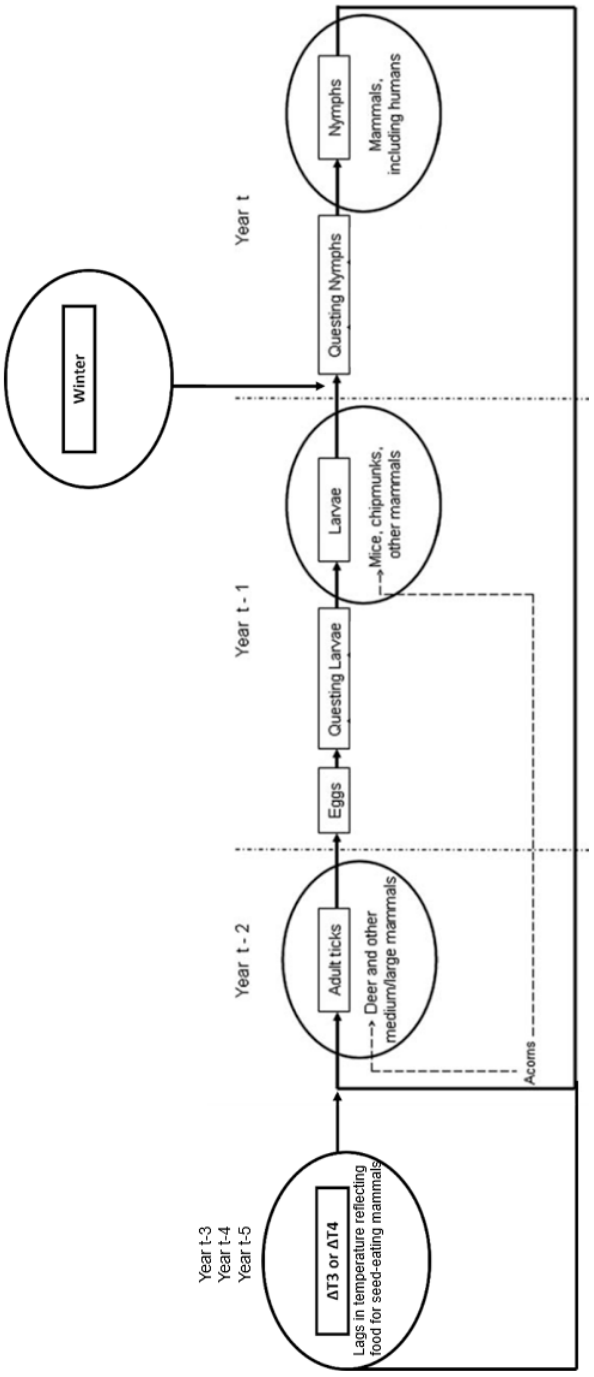

Figure 1. Diagram adapted from Ostfeld et al. 2006 showing four life stages of a tick, egg, larva, nymph, adult and environmental, and biotic factors that may have an influence in their life cycle. Year t is the focal year for this research.

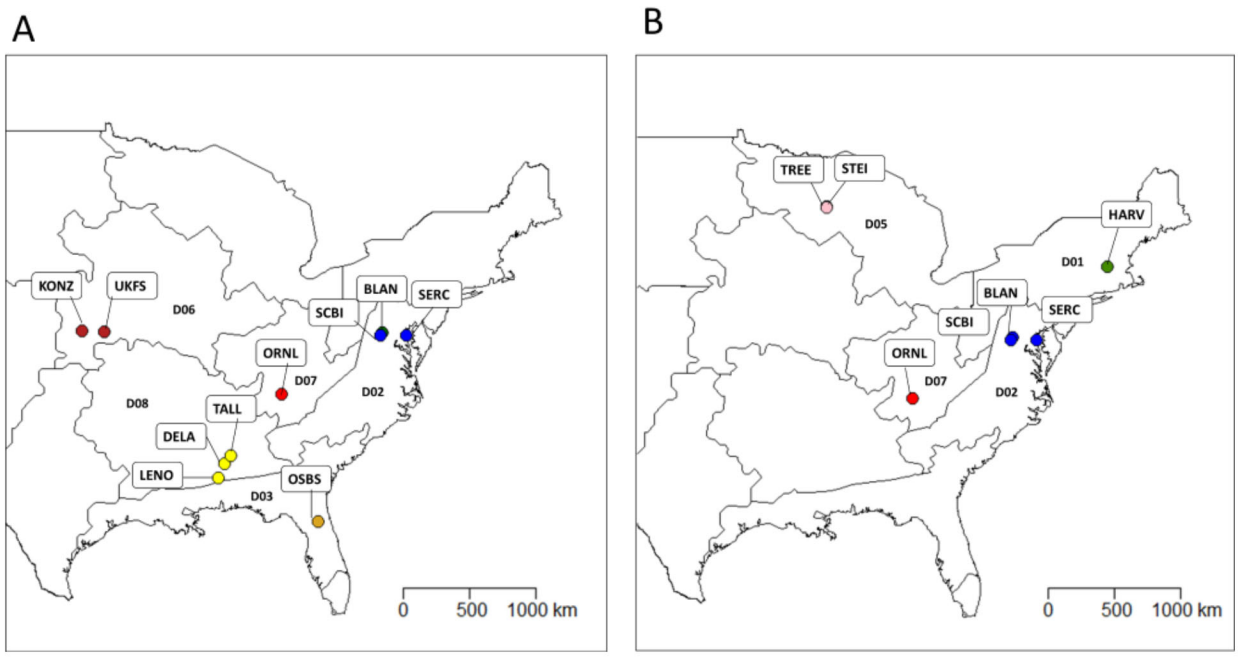

Figure 2. Map of sites used for A) *A. americanum* and B) *I. scapularis* for analyses with nymph and pathogen data between 2014-2021. Labels show NEON sites, and the outlines encompass NEON Domains. The NEON Domains included in this study are: D01-Northeast, D02-Mid-Atlantic, D03-Southeast, D05-Great Lakes, D06-Prairie Peninsula, D07-Appalachians & Cumberland Plateau, and D08-Ozarks Complex.

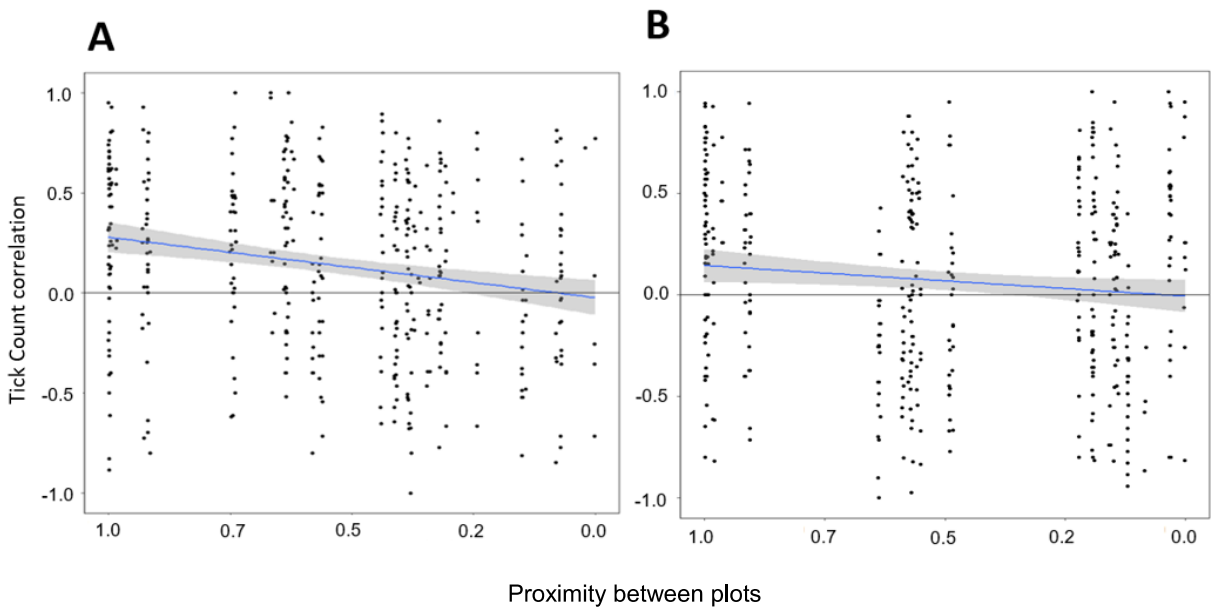

Figure 3. Spatial synchrony of nymph abundance declines with increasing proximity between NEON plots for A) *A. americanum* (0.2-1,735.0 km apart) and B) *I. scapularis* (0.2-1,476.6 km apart). Individual values are plotted as black symbols, and a regression line was drawn. Gray horizontal line drawn at zero represents no spatial synchrony. Note that proximity was calculated using distance between plots and is rescaled to range from 1 (closest together) to 0 (locations farthest apart).

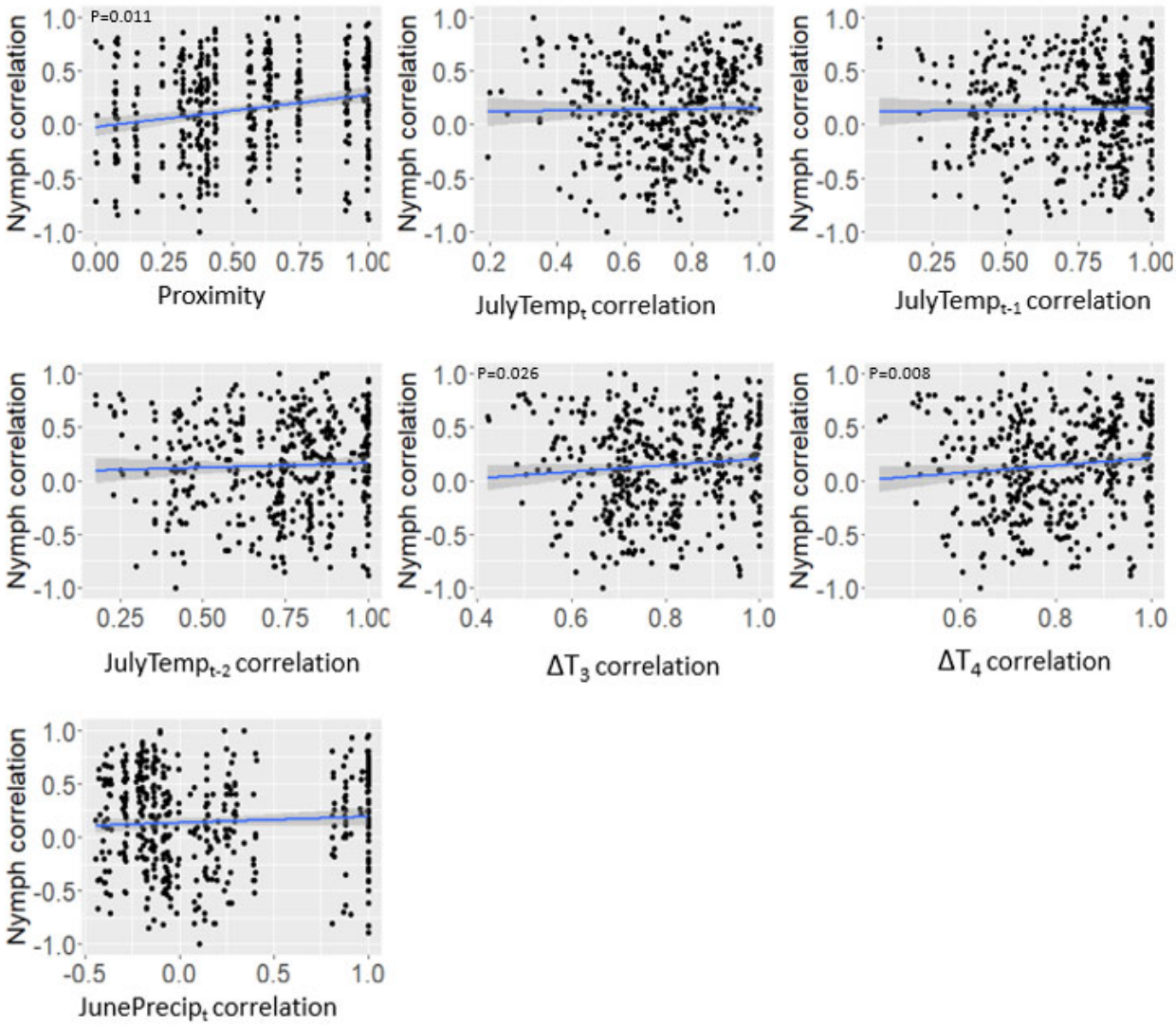

Figure 4. Relationships between synchrony of *Amblyomma americanum* tick abundance in year t calculated using Spearman correlation between pairs of NEON distributed sampling plots, the proximity between plots, and the pairwise correlation of weather factors, reflecting MRM results. Note that proximity was calculated using distance between plots and is rescaled to range from 0 (locations farthest apart) to 1 (closest together), and all other plots have correlations on the x-axis and could range from -1 to +1. P values are shown when the variable was significant in an MRM model.

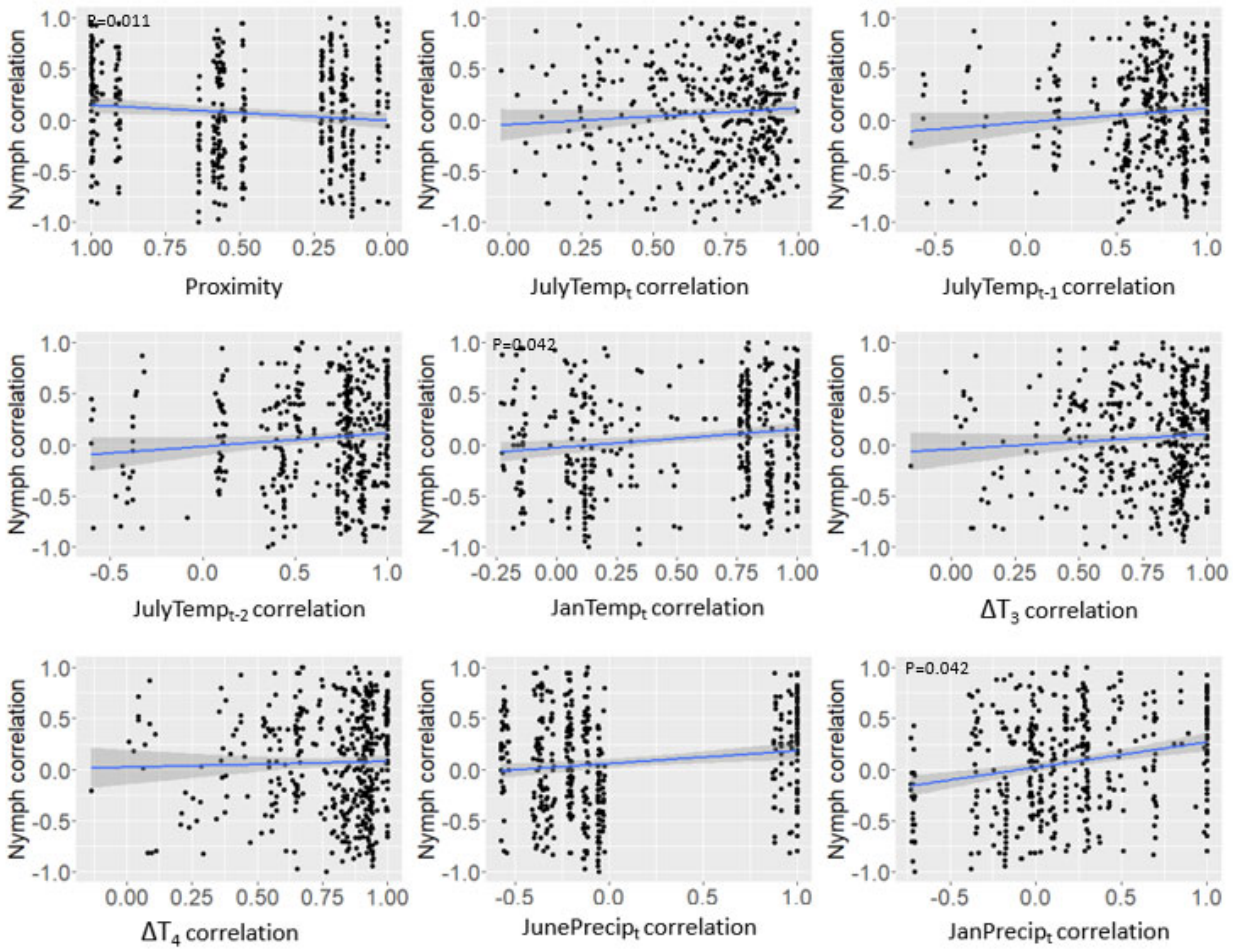

Figure 5. Relationships between synchrony of *Ixodes scapularis* tick abundance in year t calculated using Spearman correlation between pairs of NEON distributed sampling plots, the proximity between plots, and the pairwise correlation of weather factors, reflecting MRM results. Note that proximity was calculated using distance between plots and is rescaled to range from 0 (locations farthest apart) to 1 (closest together), and all other plots have correlations on the x-axis and could range from -1 to +1. P values are shown when the variable was significant in an MRM model or they were terms in an MRM model that was significant overall.

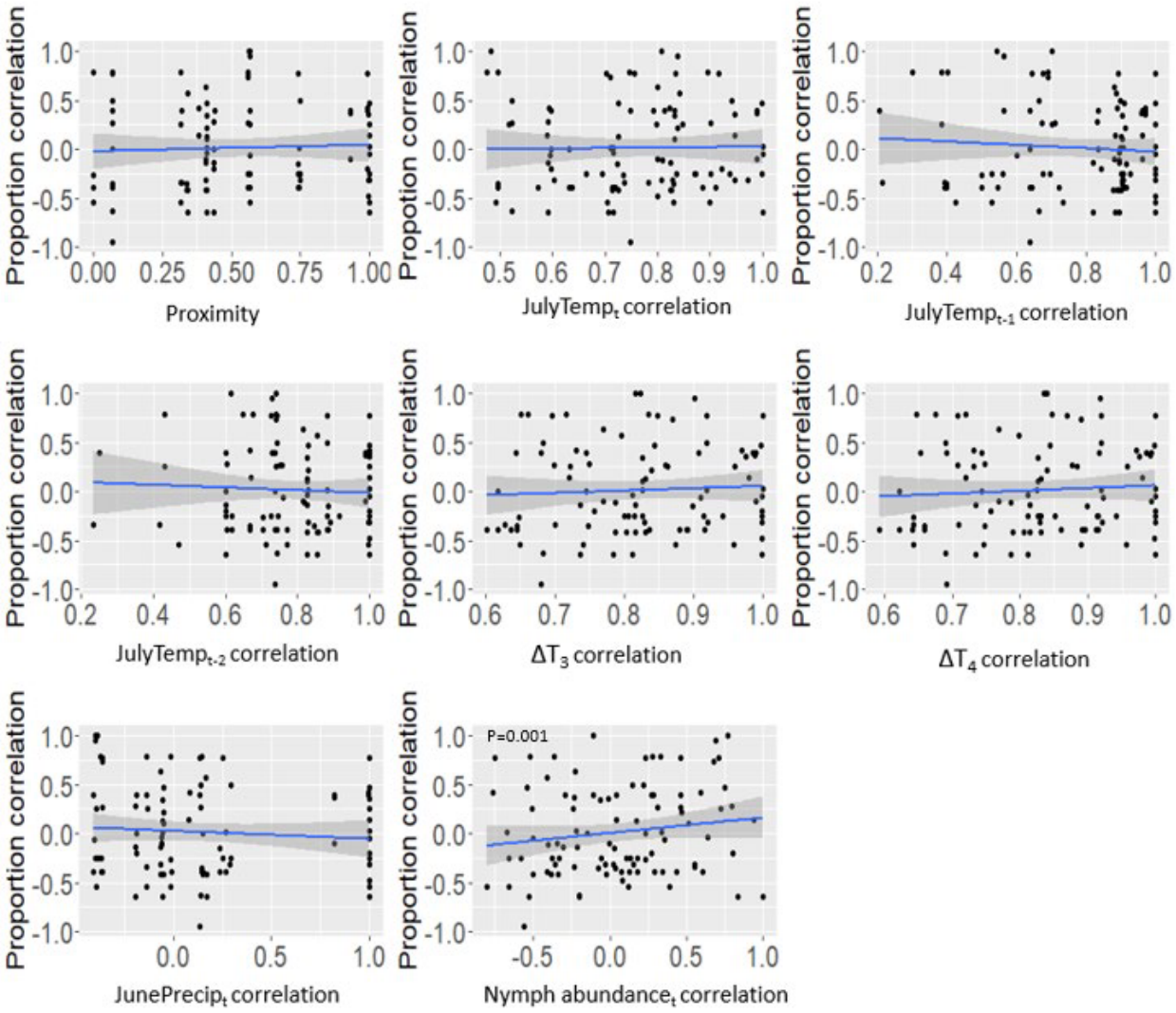

Figure 6. Relationships between synchrony of *Amblyomma americanum* proportion of infection in year t calculated using Spearman correlation between pairs of NEON distributed sampling plots, the proximity between plots, and the pairwise correlation of weather factors, reflecting MRM results. Note that proximity was calculated using distance between plots and is rescaled to range from 0 (locations farthest apart) to 1 (closest together), and all other plots have correlations on the x-axis and could range from -1 to +1. P values are shown when the variable was significant in an MRM model.

References

Asif, Z., Chen, Z., Sadiq, R., & Zhu, Y. (2023). Climate Change Impacts on Water Resources and Sustainable Water Management Strategies in North America. *Water Resources Management*. https://doi.org/10.1007/s11269-023-03474-4

Barbour, A. G., Adeolu, M., & Gupta, R. S. (2017). Division of the genus *Borrelia* into two genera (corresponding to Lyme disease and relapsing fever groups) reflects their genetic and phenotypic distinctiveness and will lead to a better understanding of these two groups of microbes (Margos et al. (2016) There is inadequate evidence to support the division of the genus *Borrelia*. *International Journal of Systematic and Evolutionary Microbiology*, *67*(6), 2058–2067. https://doi.org/10.1099/ijsem.0.001815

Barton, K. (2020). MuMIn: Multi-Model Inference. In *Version* (R package version 1.43.17; Vol. 1, Issue 18). https://CRAN.R-project.org/package=MuMIn

Bogdziewicz, M., Zwolak, R., & Crone, E. E. (2016). How do vertebrates respond to mast seeding? *Oikos*, *125*(3), 300–307. https://doi.org/10.1111/oik.03012

Borgmann-Winter, B. W., Oggenfuss, K. M., & Ostfeld, R. S. (2021). Blacklegged tick population synchrony between oak forest and non-oak forest. *Ecological Entomology*, *46*(4), 827–833. https://doi.org/10.1111/een.13019

Bouzek, D. C., Foré, S. A., Bevell, J. G., & Kim, H.-J. (2013). A conceptual model of the *Amblyomma americanum* life cycle in northeast Missouri. *Journal of Vector Ecology*, *38*(1), 74–81. https://doi.org/10.1111/j.1948-7134.2013.12011.x

Brooks, M. E., Kristensen, K., van Benthem, K. J., Magnusson, A., Berg, C. W., Nielsen, A., Skaug, H. J., Mächler, M., & Bolker, B. M. (2017). *Modeling zero-inflated count data with glmmTMB* [Preprint]. Ecology. https://doi.org/10.1101/132753

Brooks, M. E., Kristensen, K., Darrigo, M. R., Rubim, P., Uriarte, M., Bruna, E., & Bolker, B. M. (2019). Statistical modeling of patterns in annual reproductive rates. *Ecology*, *100*(7). https://doi.org/10.1002/ecy.2706

Brooks, M., Bolker, B., Kristensen, K., & Maechler, M. (2023). Package 'glmmTMB'.

Burgdorfer, W., Barbour, A. G., Hayes, S., Benach, J., Grunnwaldt, E., & Davis, J. P. (1982). *Lyme Disease—A Tick-Borne Spirochetosis?*

Burtis, J. C., Sullivan, P., Levi, T., Oggenfuss, K., Fahey, T. J., & Ostfeld, R. S. (2016). The impact of temperature and precipitation on blacklegged tick activity and Lyme disease incidence in endemic and emerging regions. *Parasites & Vectors*, *9*(1), 606. https://doi.org/10.1186/s13071-016-1894-6

Burnham, K. P., & Anderson, D. R. (2004). Multimodel inference: understanding AIC and BIC in model selection. *Sociological methods & research*, *33*(2), 261-304.

CDC, last edited 2019. *Lyme and other Tickborne Diseases Increasing.* Centers for Disease Control and Prevention. https://www.cdc.gov/media/dpk/diseases-and-conditions/lyme-disease/index.html

Dong, Y., Huang, Z., Zhang, Y., Wang, Y. X. G., & La, Y. (2020). Comparing the Climatic and Landscape Risk Factors for Lyme Disease Cases in the Upper Midwest and Northeast United States. *International Journal of Environmental Research and Public Health*, *17*(5), 1548. https://doi.org/10.3390/ijerph17051548

Eisen, R. J., Kugeler, K. J., Eisen, L., Beard, C. B., & Paddock, C. D. (2017). Tick-Borne Zoonoses in the United States: Persistent and Emerging Threats to Human Health. *ILAR Journal*, *58*(3), 319–335. https://doi.org/10.1093/ilar/ilx005

Elkinton, J. S., Liebhold, A. M., & Muzika, R.-M. (2004). Effects of alternative prey on predation by small mammals on gypsy moth pupae. *Population Ecology*, *46*(2). https://doi.org/10.1007/s10144-004-0175-y

Elmendorf, S., & Thibault, K. (n.d.). *NEON USER GUIDE TO TICKS SAMPLED USING DRAG CLOTHS (NEON.DP1.10093)*. 10.

Goslee, S. C., & Urban, D. L. (2007). The **ecodist** Package for Dissimilarity-based Analysis of Ecological Data. *Journal of Statistical Software*, *22*(7). https://doi.org/10.18637/jss.v022.i07

Granter, S. R., Bernstein, A., & Ostfeld, R. S. (2014). Of Mice and Men: Lyme Disease and Biodiversity. *Perspectives in Biology and Medicine*, *57*(2), 198–207. https://doi.org/10.1353/pbm.2014.0015

Gray, J. S., & Ogden, N. H. (2021). Ticks, Human Babesiosis and Climate Change. *Pathogens*, *10*(11), 1430. https://doi.org/10.3390/pathogens10111430

Hacket-Pain, A., Foest, J. J., Pearse, I. S., LaMontagne, J. M., Koenig, W. D., Vacchiano, G., & Ascoli, D. (2022). MASTREE+: Time-series of plant reproductive effort from six continents. *Global change biology*, *28*(9), 3066-3082

Hayes, L. E., Scott, J. A., & Stafford, K. C. (2015). Influences of weather on Ixodes scapularis nymphal densities at long-term study sites in Connecticut. *Ticks and Tick-Borne Diseases*, *6*(3), 258–266. https://doi.org/10.1016/j.ttbdis.2015.01.006

Holland, E. P., James, A., Ruscoe, W. A., Pech, R. P., & Byrom, A. E. (2015). Climate-Based Models for Pulsed Resources Improve Predictability of Consumer Population Dynamics: Outbreaks of House Mice in Forest Ecosystems. *PLOS ONE*, *10*(3), e0119139. https://doi.org/10.1371/journal.pone.0119139

Horobik, V., Keesing, F., & Ostfeld, R. S. (2007). Abundance and *Borrelia burgdorferi*-infection Prevalence of Nymphal Ixodes scapularis Ticks along Forest–Field Edges. *EcoHealth*, *3*(4), 262–268. https://doi.org/10.1007/s10393-006-0065-1

Jackson, W. L. (2018). Mammalian meat allergy following a tick bite: A case report. *Oxford Medical Case Reports*, *2018*(2). https://doi.org/10.1093/omcr/omx098

Janzen, D. H. (1971). Seed Predation by Animals. *Annual Review of Ecology and Systematics*, *2*(1), 465–492. https://doi.org/10.1146/annurev.es.02.110171.002341

Jones, K. E., Patel, N. G., Levy, M. A., Storeygard, A., Balk, D., Gittleman, J. L., & Daszak, P. (2008). Global trends in emerging infectious diseases. *Nature*, *451*(7181), 990–993. https://doi.org/10.1038/nature06536

Kao, R. H., Gibson, C. M., Gallery, R. E., Meier, C. L., Barnett, D. T., Docherty, K. M., & Schimel, D. (2012). NEON terrestrial field observations: designing continental-scale, standardized sampling. *Ecosphere*, *3*(12), 1-17.

Karasuyama, H., Miyake, K., & Yoshikawa, S. (2020). Immunobiology of Acquired Resistance to Ticks. *Frontiers in Immunology*, *11*, 601504. https://doi.org/10.3389/fimmu.2020.601504

Karesh, W. B., Dobson, A., Lloyd-Smith, J. O., Lubroth, J., Dixon, M. A., Bennett, M., Aldrich, S., Harrington, T., Formenty, P., Loh, E. H., Machalaba, C. C., Thomas, M. J., & Heymann, D. L. (2012). Ecology of zoonoses: Natural and unnatural histories. *The Lancet*, *380*(9857), 1936–1945. https://doi.org/10.1016/S0140-6736(12)61678-X

Kelly, D., Koenig, W. D., & Liebhold, A. M. (2008). An intercontinental comparison of the dynamic behavior of mast seeding communities. *Population Ecology*, *50*(4), 329–342. https://doi.org/10.1007/s10144-008-0114-4

Kelly, D., Geldenhuis, A., James, A., Penelope Holland, E., Plank, M. J., Brockie, R. E., Cowan, P. E., Harper, G. A., Lee, W. G., Maitland, M. J., Mark, A. F., Mills, J. A., Wilson, P. R., & Byrom, A. E. (2013). Of mast and mean: Differential-temperature cue makes mast seeding insensitive to climate change. *Ecology Letters*, *16*(1), 90–98. https://doi.org/10.1111/ele.12020

Koenig, W. D. (2002). Global patterns of environmental synchrony and the Moran effect. *Ecography*, *25*(3), 283–288. https://doi.org/10.1034/j.1600-0587.2002.250304.x

Kugeler, K. J., Farley, G. M., Forrester, J. D., & Mead, P. S. (2015). Geographic Distribution and Expansion of Human Lyme Disease, United States. Emerging Infectious Diseases, 21(8), 1455–1457. https://doi.org/10.3201/eid2108.141878

LaMontagne, J. M., Pearse, I. S., Greene, D. F., & Koenig, W. D. (2020). Mast seeding patterns are asynchronous at a continental scale. Nature Plants, 6(5), 460–465. https://doi.org/10.1038/s41477-020-0647-x

LaMontagne, J. M., Redmond, M. D., Wion, A. P., & Greene, D. F. (2021). An assessment of temporal variability in mast seeding of North American Pinaceae. Philosophical Transactions of the Royal Society B: Biological Sciences, 376(1839), 20200373. https://doi.org/10.1098/rstb.2020.0373

Levan,K.,(2019). TOS Protocol and Procedure: Tick and Tick-Borne Pathogen Sampling. 57

Ledger, K. J., Keenan, R. M., Sayler, K. A., & Wisely, S. M. (2019). Multi-scale patterns of tick occupancy and abundance across an agricultural landscape in southern Africa. *PLOS ONE*, *14*(9), e0222879. https://doi.org/10.1371/journal.pone.0222879

Levi, T., Keesing, F., Oggenfuss, K., & Ostfeld, R. S. (2015). Accelerated phenology of blacklegged ticks under climate warming. *Philosophical Transactions of the Royal Society B: Biological Sciences*, *370*(1665), 20130556. https://doi.org/10.1098/rstb.2013.0556

Li, D., Record, S., Sokol, E. R., Bitters, M. E., Chen, M. Y., Chung, Y. A., Helmus, M. R., Jaimes, R., Jansen, L., Jarzyna, M. A., Just, M. G., LaMontagne, J. M., Melbourne, B. A., Moss, W., Norman, K. E. A., Parker, S. M., Robinson, N., Seyednasrollah, B., Smith, C., … Zarnetske, P. L. (2022). Standardized NEON organismal data for biodiversity research. *Ecosphere*, *13*(7). https://doi.org/10.1002/ecs2.4141

Liebhold, A., Koenig, W. D., & Bjørnstad, O. N. (2004). Spatial Synchrony in Population Dynamics. *Annual Review of Ecology, Evolution, and Systematics*, *35*(1), 467–490. https://doi.org/10.1146/annurev.ecolsys.34.011802.132516

LoGiudice, K., Ostfeld, R. S., Schmidt, K. A., & Keesing, F. (2003). The ecology of infectious disease: Effects of host diversity and community composition on Lyme disease risk. *Proceedings of the National Academy of Sciences*, *100*(2), 567–571. https://doi.org/10.1073/pnas.0233733100

Lüdecke, D., Makowski, D., Waggoner, P., & Patil, I. (2019). Package 'performance.'

McCabe, G. J., & Bunnell, J. E. (2004). Precipitation and the Occurrence of Lyme Disease in the Northeastern United States. *Vector-Borne and Zoonotic Diseases*, *4*(2), 143–148. https://doi.org/10.1089/1530366041210765

Mangan, M. J., Foré, S. A., & Kim, H. J. (2018). Ecological modeling over seven years to describe the number of hosts-seeking *Amblyomma americanum* in each life stage in northeast Missouri. *Journal of Vector Ecology*, *43*(2), 271-284.

Mixson, T. R., Campbell, S. R., Gill, J. S., Ginsberg, H. S., Reichard, M. V., Schulze, T. L., & Dasch, G. A. (2006). Prevalence of Ehrlichia, Borrelia, and Rickettsial Agents in *Amblyomma americanum* (Acari: Ixodidae) Collected from Nine States. *JOURNAL OF MEDICAL ENTOMOLOGY*, *43*(6).

Moran, P. A. 1953. The statistical analysis of the Canadian lynx cycle. II. Synchronization and meteorology. Australian Journal of Zoology 1:291–298.

Ostfeld, R. S., Cepeda, O. M., Hazler, K. R., & Miller, M. C. (1995). Ecology of Lyme Disease: Habitat Associations of Ticks (*Ixodes Scapularis*) In a Rural Landscape. *Ecological Applications*, *5*(2), 353–361. https://doi.org/10.2307/1942027

Ostfeld, R. S., Schauber, E. M., Canham, C. D., Keesing, F., Jones, C. G., & Wolff, J. O. (2001). Effects of Acorn Production and Mouse Abundance on Abundance and *Borrelia burgdorferi* Infection Prevalence of Nymphal *Ixodes scapularis* Ticks. *Vector-Borne and Zoonotic Diseases*, *1*(1), 55–63. https://doi.org/10.1089/153036601750137688

Ostfeld, R. S., Canham, C. D., Oggenfuss, K., Winchcombe, R. J., & Keesing, F. (2006). Climate, Deer, Rodents, and Acorns as Determinants of Variation in Lyme-Disease Risk. *PLoS Biology*, *4*(6), e145. https://doi.org/10.1371/journal.pbio.0040145

Parola, P., & Raoult, D. (2001). Ticks and Tickborne Bacterial Diseases in Humans: An Emerging Infectious Threat. *Clinical Infectious Diseases*, *32*(6), 897–928. https://doi.org/10.1086/319347

Paddock, C. D., & Yabsley, M. J. (2007). Ecological Havoc, the Rise of White-Tailed Deer, and the Emergence of *Amblyomma americanum*-Associated Zoonoses in the United States. In J. E. Childs, J. S. Mackenzie, & J. A. Richt (Eds.), *Wildlife and Emerging Zoonotic Diseases: The Biology, Circumstances and Consequences of Cross-Species Transmission* (Vol. 315, pp. 289–324). Springer Berlin Heidelberg. https://doi.org/10.1007/978-3-540-70962-6_12

Paull, S. H., Thibault, K. M., & Benson, A. L. (2022). Tick abundance, diversity and pathogen data collected by the National Ecological Observatory Network. *Gigabyte*, *2022*, 1–11. https://doi.org/10.46471/gigabyte.56

Pearse, I. S., Koenig, W. D., & Kelly, D. (2016). Mechanisms of mast seeding: Resources, weather, cues, and selection. *New Phytologist*, *212*(3), 546–562. https://doi.org/10.1111/nph.14114

Pearse, I. S., LaMontagne, J. M., & Koenig, W. D. (2017). Inter-annual variation in seed production has increased over time (1900–2014). *Proceedings of the Royal Society B: Biological Sciences*, *284*(1868), 20171666. https://doi.org/10.1098/rspb.2017.1666

Pfäffle, M., Littwin, N., Muders, S. V., & Petney, T. N. (2013). The ecology of tick-borne diseases. *International Journal for Parasitology*, *43*(12–13), 1059–1077. https://doi.org/10.1016/j.ijpara.2013.06.009

Rand, P. W., Lubelczyk, C., Lavigne, G. R., Elias, S., Holman, M. S., Lacombe, E. H., & Smith, R. P. (2003). Deer Density and the Abundance of *Ixodes scapularis* (Acari: Ixodidae). *Journal of Medical Entomology*, *40*(2), 179–184. https://doi.org/10.1603/0022-2585-40.2.179

Randolph, S. E., Green, R. M., Hoodless, A. N., & Peacey, M. F. (2002). An empirical quantitative framework for the seasonal population dynamics of the tick *Ixodes ricinus*. *International Journal for Parasitology*, *32*(8), 979–989. https://doi.org/10.1016/S0020-7519(02)00030-9

Ranta, E., Kaitala, V., Lindström, J., Helle, E., & Lindstrom, J. (1997). The Moran Effect and Synchrony in Population Dynamics. *Oikos*, *78*(1), 136. https://doi.org/10.2307/3545809

Roland, W. E., McDonald, G., Caldwell, C. W., & Everett, E. D. (1995). Ehrlichiosis—a cause of prolonged fever. *Clinical infectious diseases*, *20*(4), 821-825.

Ruiz-Fons, F., Fernández-de-Mera, I. G., Acevedo, P., Gortázar, C., & De La Fuente, J. (2012). Factors Driving the Abundance of *Ixodes ricinus* Ticks and the Prevalence of Zoonotic I. ricinus-Borne Pathogens in Natural Foci. *Applied and Environmental Microbiology*, *78*(8), 2669–2676. https://doi.org/10.1128/AEM.06564-11

Schulze, T. L., Jordan, R. A., Schulze, C. J., & Hung, R. W. (2009). Precipitation and Temperature as Predictors of the Local Abundance of *Ixodes scapularis* (Acari: Ixodidae) Nymphs. *Journal of Medical Entomology*, *46*(5), 1025–1029. https://doi.org/10.1603/033.046.0508

Sork, V. L. (1993). Evolutionary Ecology of Mast-Seeding in Temperate and Tropical Oaks (Quercus spp.). *Vegetatio*, *107/108*, 133–147

Spach, D. H., Liles, W. C., Campbell, G. L., Quick, R. E., Anderson Jr, D. E., & Fritsche, T. R. (1993). Tick-borne diseases in the United States. *New England Journal of Medicine*, *329*(13), 936-947.

Swei, A., Couper, L. I., Coffey, L. L., Kapan, D., & Bennett, S. (2020). Patterns, Drivers, and Challenges of Vector-Borne Disease Emergence. *Vector-Borne and Zoonotic Diseases*, *20*(3), 159–170. https://doi.org/10.1089/vbz.2018.2432

Zuckerberg, B., Strong, C., LaMontagne, J. M., St. George, S., Betancourt, J. L., & Koenig, W. D. (2020). Climate Dipoles as Continental Drivers of Plant and Animal Populations. Trends in Ecology & Evolution, 35(5), 440–453. https://doi.org/10.1016/j.tree.2020.01.010

Wang, T., Hamann, A., Spittlehouse, D., & Carroll, C. (2016). Locally Downscaled and Spatially Customizable Climate Data for Historical and Future Periods for North America. *PLOS ONE*, *11*(6), e0156720. https://doi.org/10.1371/journal.pone.0156720

Whitlow, A. M., Schürch, R., Mullins, D., & Eastwood, G. (2021). The Influence of Southwestern Virginia Environmental Conditions on the Potential Ability of *Haemaphysalis longicornis*, *Amblyomma americanum*, and *Amblyomma maculatum* to Overwinter in the Region. *Insects*, *12*(11), 1000. https://doi.org/10.3390/insects12111000

Yang, L. H., Bastow, J. L., Spence, K. O., & Wright, A. N. (2008). What can we learn from resource pulses? *Ecology*, *89*(3), 621-634.

Appendices

Table A1. NEON Domains and sites included in AICc analysis located in the United States. Mean average temperature and standard deviation was calculated based on mean temperature of NEON sites. The number of years included a span of 13 years.

NEON Domain	Location	Mean Temperature (°C)	SD Temperature (°C)	NEON Sites
D01-Northeast	Massachusetts	20.26	2.70	HARV
D02-Mid-Atlantic	Virginia and Maryland	24.85	1.84	BLAN, SCBI, SERC
D03-Southeast	Florida	27.71	0.51	OSBS
D05-Great Lakes	Wisconsin	19.31	1.60	STEI, TREE
D06-Prairie Peninsula	Kansas	25.97	1.72	UKFS
D07-Appalachians & Cumberland Plateau	Tennessee	25.12	1.64	ORNL
D08-Ozarks Complex	Alabama	26.98	1.13	DELA, LENO, TALL

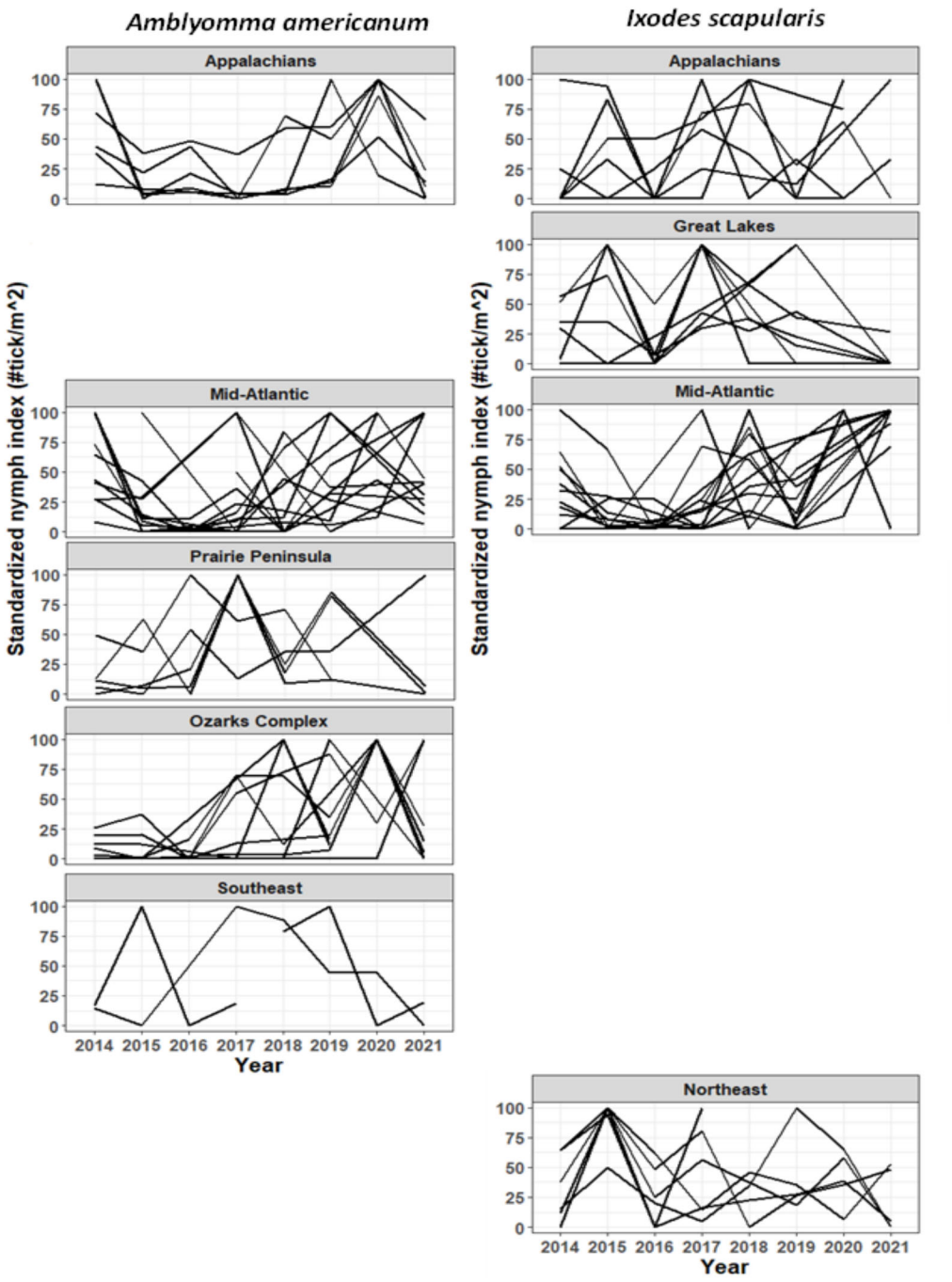

Figure A1. Standardized population size of the mean density of tick nymphs across years (between 0 to 100) for NEON Domains with forest land cover type. Each line corresponds to data from a distributed plot at NEON sites within the Domain; Domain names are indicated above each graph. Rows with the same Domain show where the distribution of the tick species overlap.

Table A2. Multiple regression on distance matrices (MRM) results for proximity, weather, and biotic factors influencing the proportion of synchrony of infected ticks for the species I. scapularis in year t.

Model & Variables	Coefficient	P (variable)	R^2 (model)	P (model)
1. Space			0.0003	0.168
Proximity	-0.019	0.168		
2. Weather: Host variables			0.0003	0.910
$JulyTemp_t$	-0.001	0.963		
$JunePrecip_t$	-0.029	0.168		
$JulyTemp_{t-1}$	0.039	0.481		
$JulyTemp_{t-2}$	-0.026	0.591		
3. Nymph abundance			0.0001	0.546
Nymphs	0.012	0.546		
4. Mast seeding variables			0.0003	0.785
ΔT_3	0.025	0.600		
ΔT_4	-0.010	0.813		
5. Saturated model			0.0002	0.847
Proximity	-0.004	0.838		
$JulyTemp_t$	-0.009	0.690		
June Precipitation	0.020	0.304		
Nymphs	0.015	0.444		
$JulyTemp_{t-1}$	0.057	0.322		
$JulyTemp_{t-2}$	-0.065	0.319		
ΔT_3	0.046	0.444		
ΔT_4	-0.012	0.793		

\

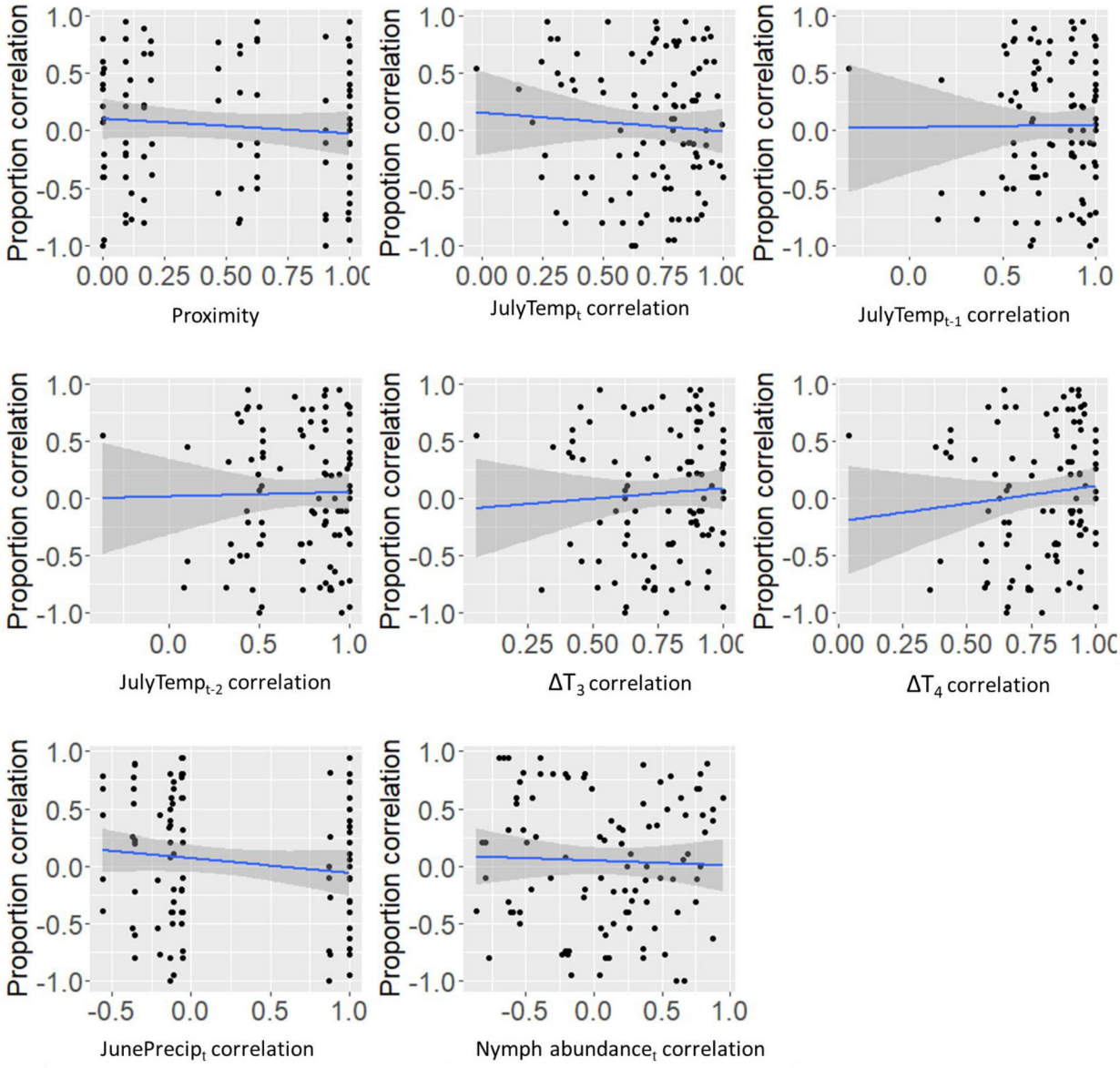

Figure A2. Relationships between synchrony of *Ixodes scapularis* proportion of infection in year t calculated using Spearman correlation between pairs of NEON distributed sampling plots, the proximity between plots, and the pairwise correlation of weather factors, reflecting MRM results. Note that proximity was calculated using distance between plots and is rescaled to range from 0 (locations farthest apart) to 1 (closest together), and all other plots have correlations on the x-axis and could range from -1 to +1. None of these variables were statistically significant in the MRM.

Figure A3. Mean of nymph abundance across years in NEON sites where *I. scapularis* and *A. americanum* overlapped for a minimum of 3 years. A) BLAN, B) ORNL, C) SCBI, and D) SERC. Red line corresponds to the species *A. americanum* and the blue line corresponds to the species *I. scapularis*. Note that BLAN and SERC are missing data for the year 2020.

Table A3. Spearman correlation between *Ixodes scapularis* and *Amblyomma americanum* for the distributed sampling plots in four NEON sites where these species overlapped for a minimum of three years.

Sites	Correlation	P-value	Years of overlap
BLAN	0.46	0.30	7
ORNL	-0.59	0.13	8
SCBI	0.69	0.06	8
SERC	0.14	0.78	7

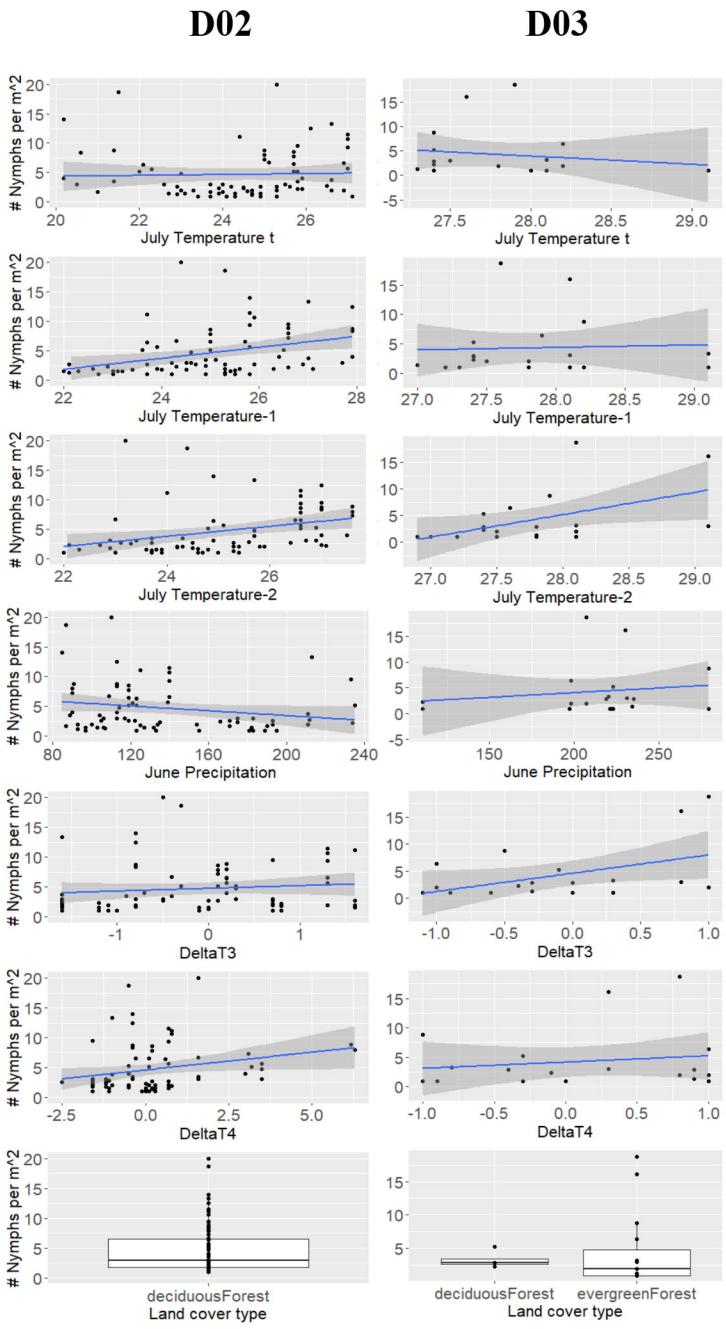

Figure A4. Part A- Relationship of *A. americanum* tick abundance and variables used in the AICc analysis for the Mid-Atlantic Domain (D02) and Southeast Domain (D03).

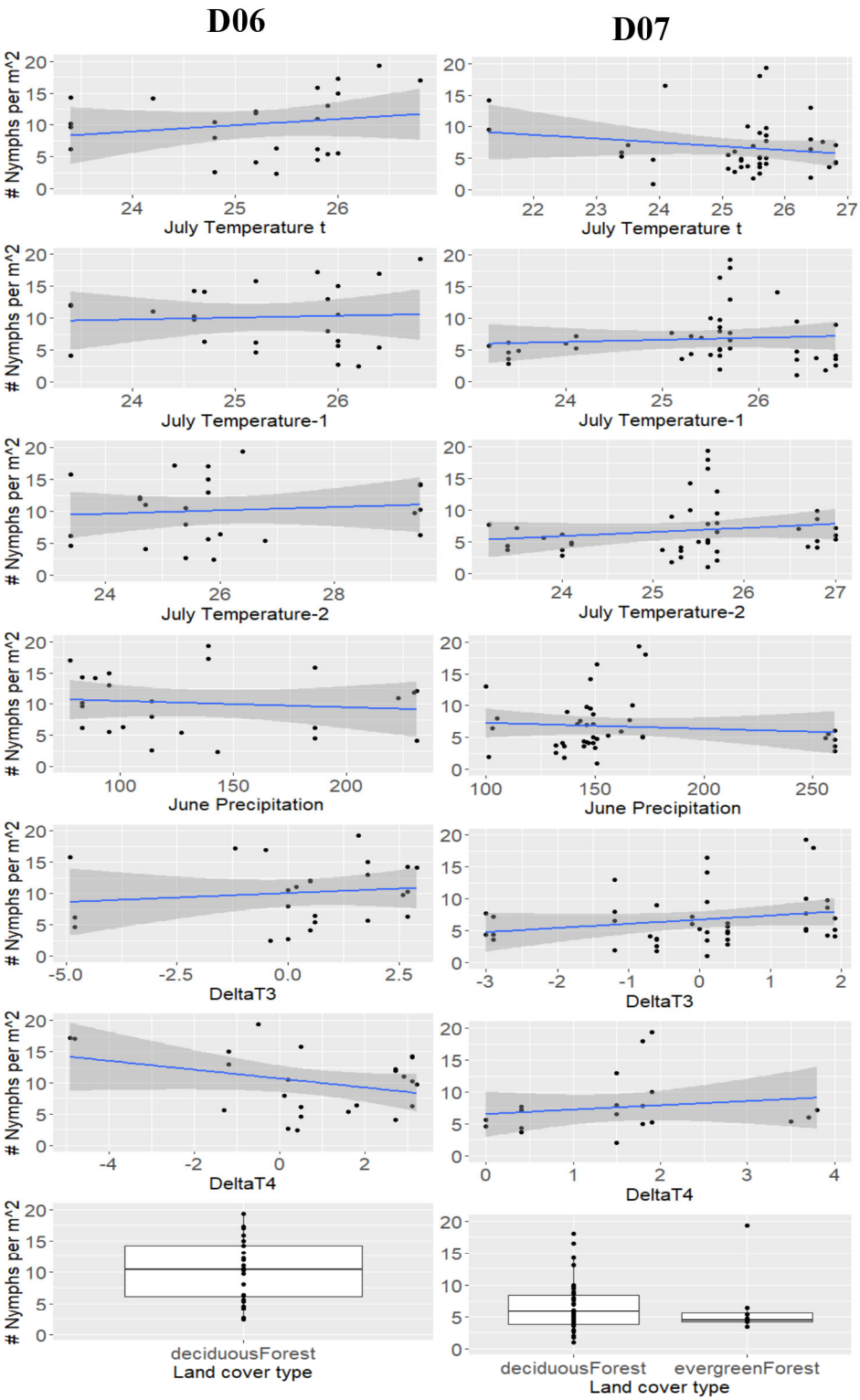

Figure A4. Part B- Relationship of *A. americanum* tick abundance and variables used in the AICc analysis for the Prairie Peninsula (D06) and Appalachians Cumberland Plateau (D07).

D08

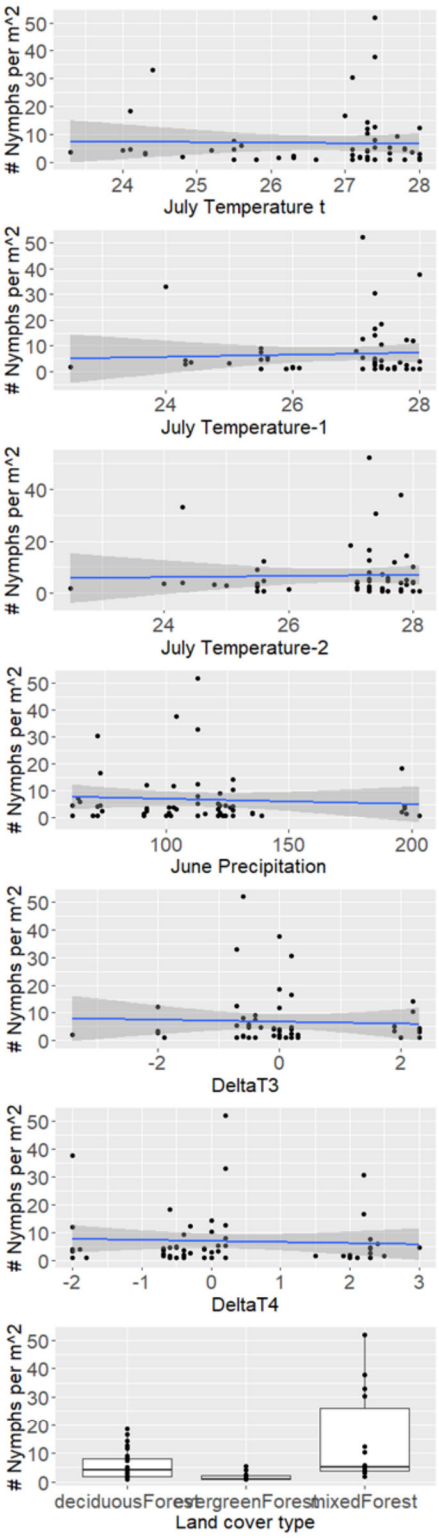

Figure A4. Part C- Relationship of *A. americanum* tick abundance and variables used in the AICc analysis for Ozarks Complex (D08).

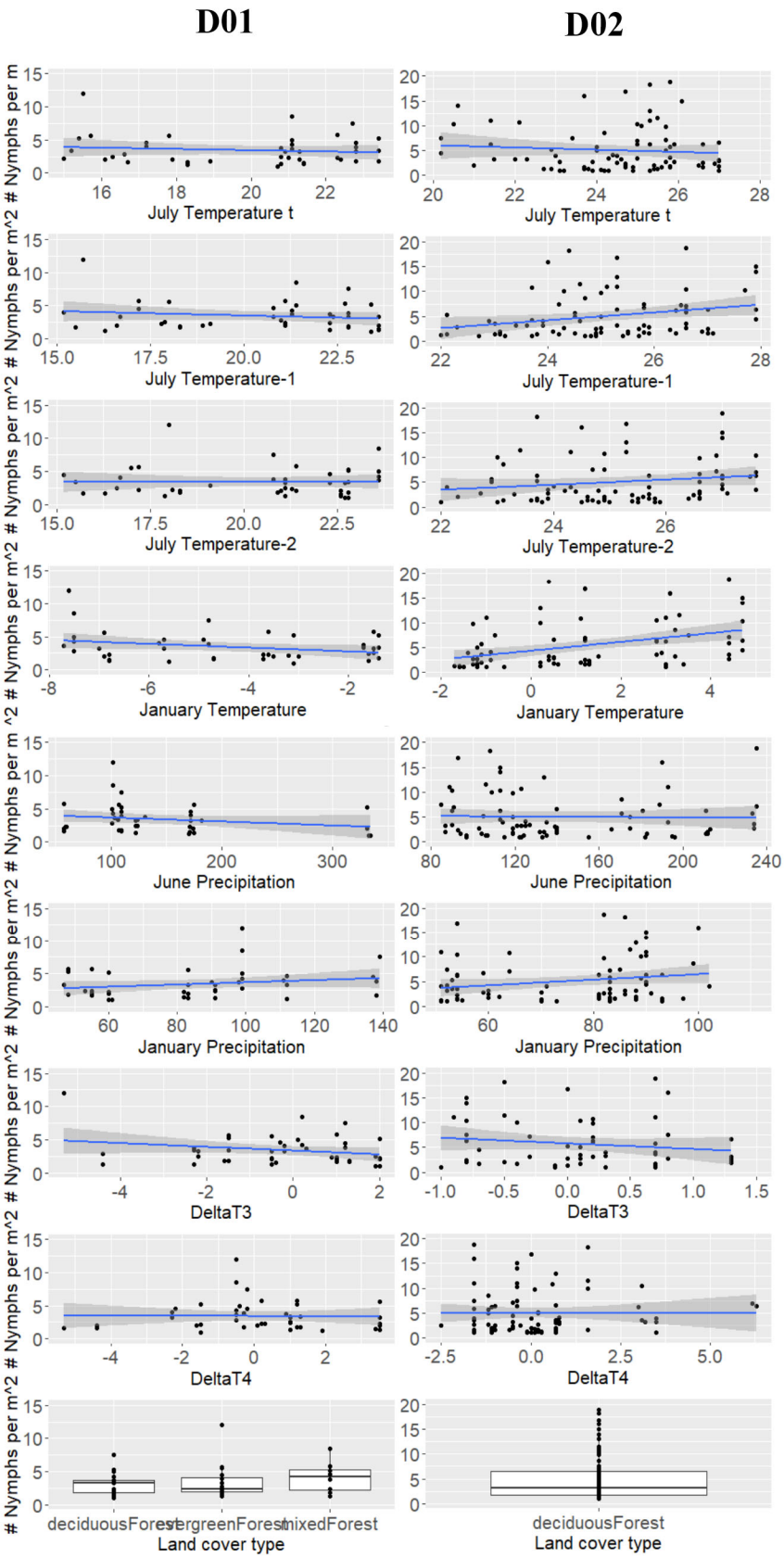

Figure A5. Part A- Relationship of *I. scapularis* tick abundance and variables used in the AICc analysis for Mid-Atlantic Domain (D01) and Northeast Domain (D02).

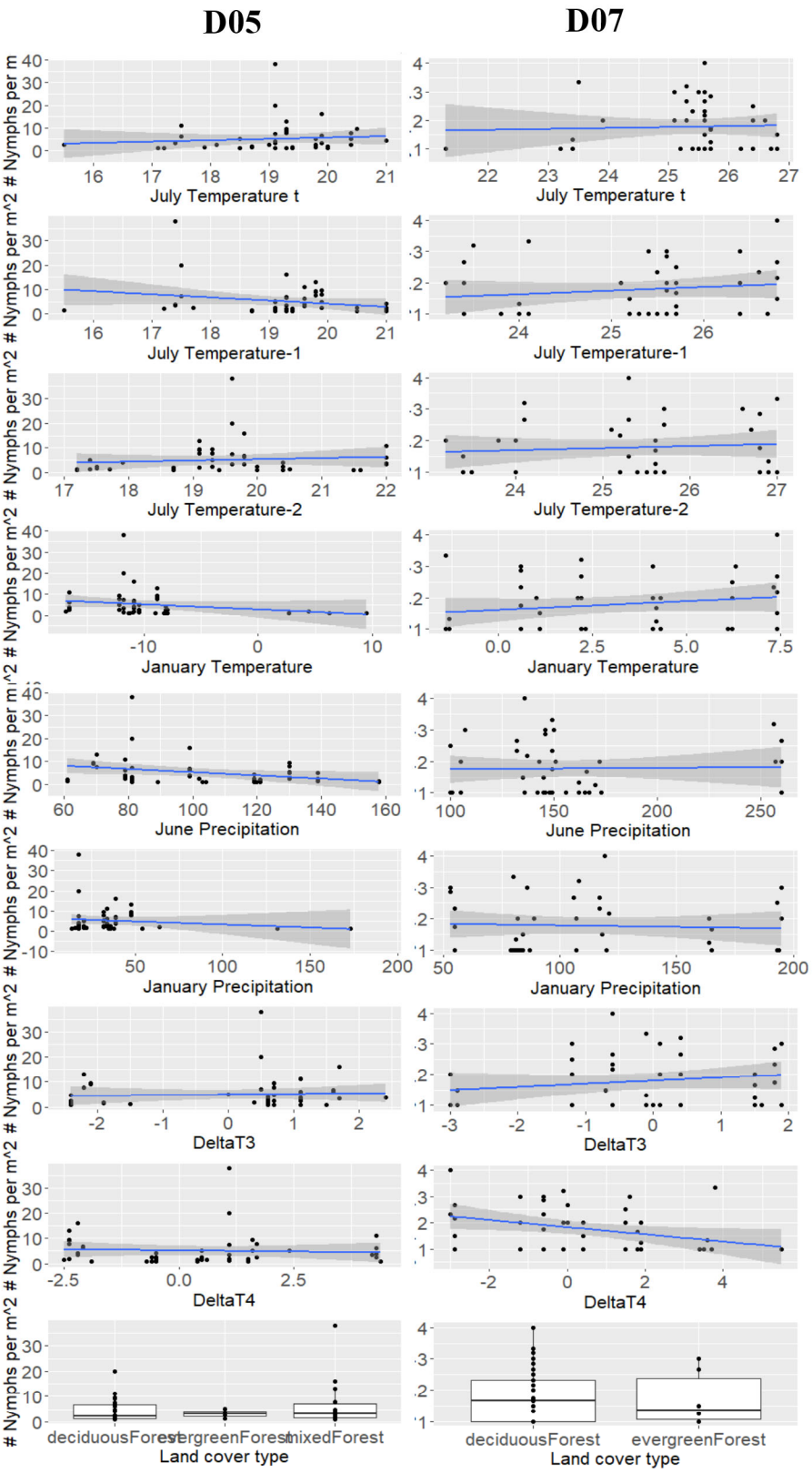

Figure A5. Part B- Relationship of I. scapularis tick abundance and variables used in the AICc analysis for Appalachians and Cumberland Plateau (D05) and Great Lakes Domain (D07).